Linac control monitors -- First direct measurement of electron and positron bunch characteristics at the positron source of the SuperKEKB B-Factory --

Tsuyoshi Suwada (*tsuyoshi.suwada@kek.jp*)
Accelerator Laboratory, KEK

Introduction

- **In 2020, the positron (*e*+) source of the *SuperKEKB* (*SKEKB*) *B-Factory* was upgraded to increase the positron yield.**
  - ***Countermeasure against electric discharge for the AMD, installations of steering magnets, and beam diagnostics.***
- **There are three difficulties to install any beam diagnostics,**
  - ***in radiation hard environment, almost no space to install them, and difficult technique to simultaneously and separately detect both secondary e- and e+ bunches with very short time interval.***
- **A wideband beam monitors (WBMs) were successfully installed in the *e*+ source.**
- **In this report, the motivation for introducing WBMs, and their detection technique, and some results are presented.**

The SKEKB e+ source

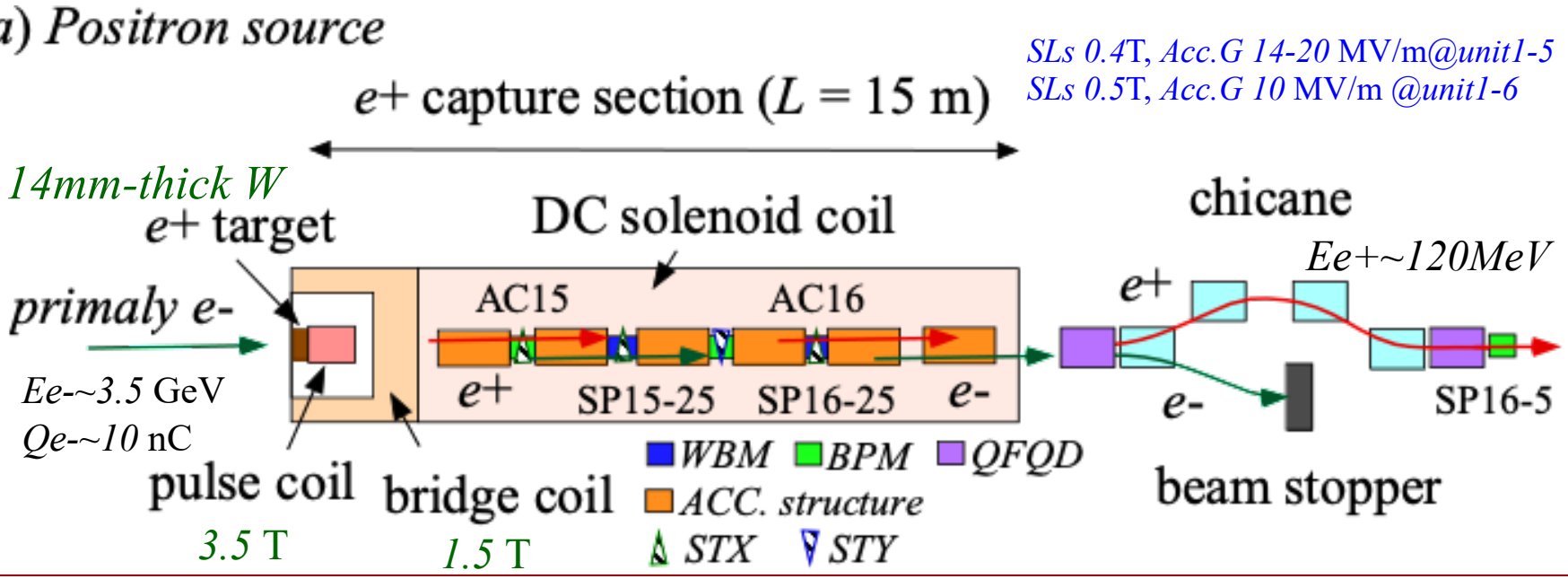

1. Secondary e+e- bunches are immediately captured in the transverse phase space by applying strong pulsed and DC magnetic fields. On the other hand, in the longitudinal direction they are captured by applying electromagnetic fields in accelerating structures. The e- bunch is stopped by a beam stopper at a chicane and the e+ bunch passes through it. The bunch charges are first measured by a standard BPM after the chicane.

2. One of the important issues for beam diagnostics is to simultaneously and separately detect parallel travelling e+e- bunches with very short distances by two WBMs in the capture section.

- *How can we detect simultaneously and separately these secondary e- and e+ bunches?*
- *Which detection technique is suitable, in time domain or frequency domain?*
- *What kinds of bunch characteristics for a single bunch are measurable?*

e- and e+ capture process in the e+ capture section through dynamical phase-slip process

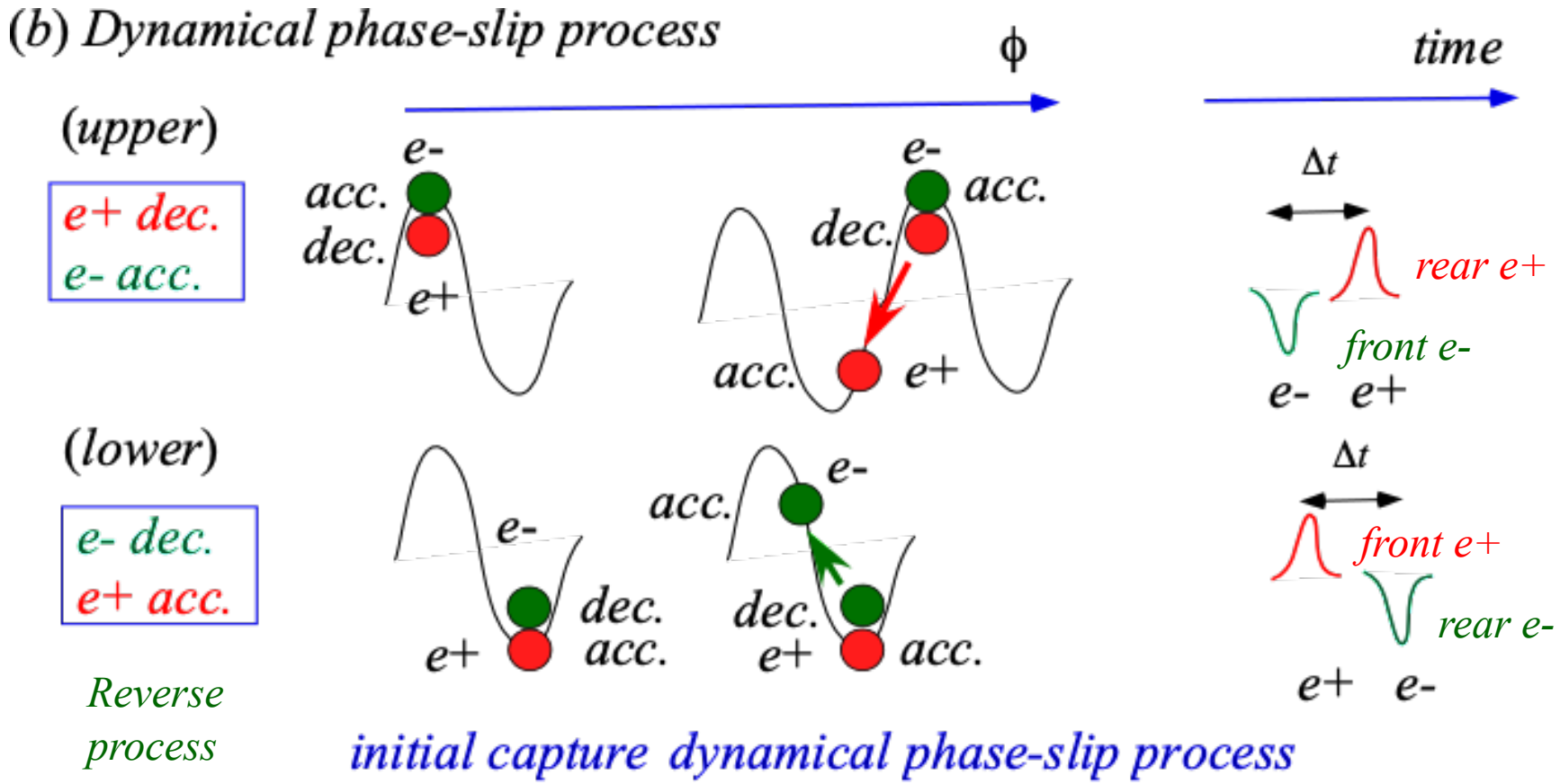

- *The line order for the e- and e+ bunches are generated with very short time intervals (Δt~ 0 - 300 ps) depending on the capture phase.*
- *To understand the dynamical capture process, it is required to precisely measure the time interval Δt between these two bunches.*

Historical detection technique in time domain at the SLC e+ sources

e+ capture section

e+ production target

Ee- ~ 33 GeV

Ne- ~ 5x10^10 e-/pulse

button pickup

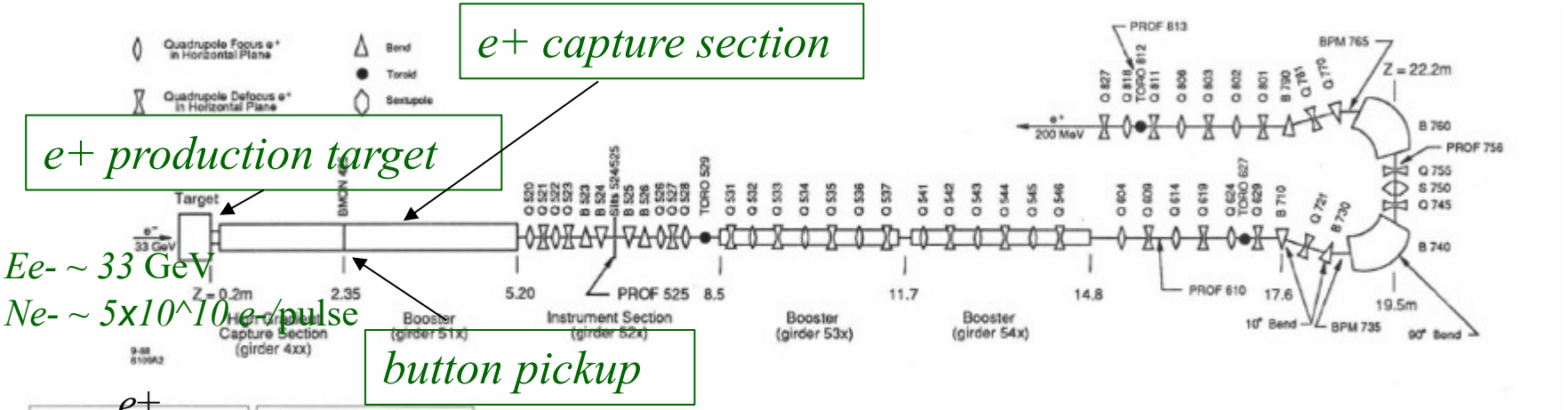

ig. 2. Positron capture and booster transport system.

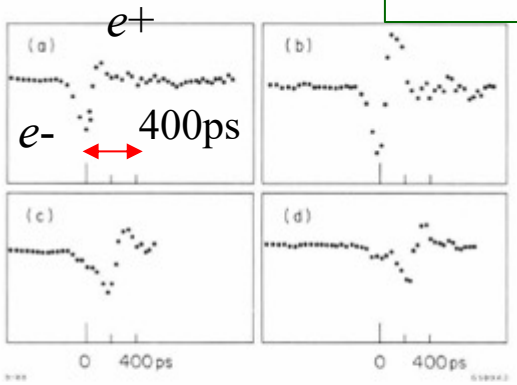

Fig. 3. Initial button monitor (BMON 425) signal: a) capture section off; b) capture RF phased (108°) for large leading negative pulse; and c) signal when RF phased about 180° away, viz., at −64° and d) at −94°.

1. Referred by J. E. Clendenin, et al., "SLC positron source startup"; Procs. of 1988 Linear Accelerator Conf, Williamsburg, Virginia, USA.

2. The commissioning of the e+ source began in early September of 1986.

We can barely recognize both e- and e+ bunches, for which the signals were obtained by a button pickup. The bunch separation is not very good in time domain.

Historical detection technique in frequency domain at the APS e+ sources

e+ production target

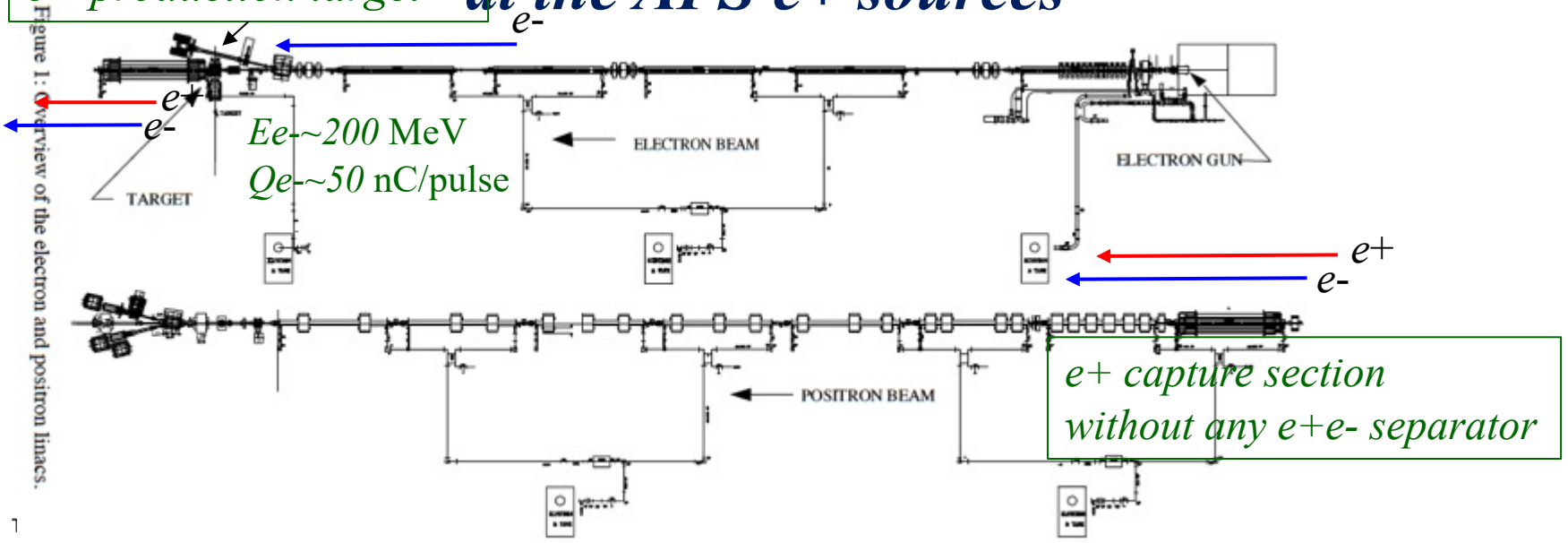

Figure 1: Overview of the electron and positron linacs.

e+ capture section
without any e+e- separator

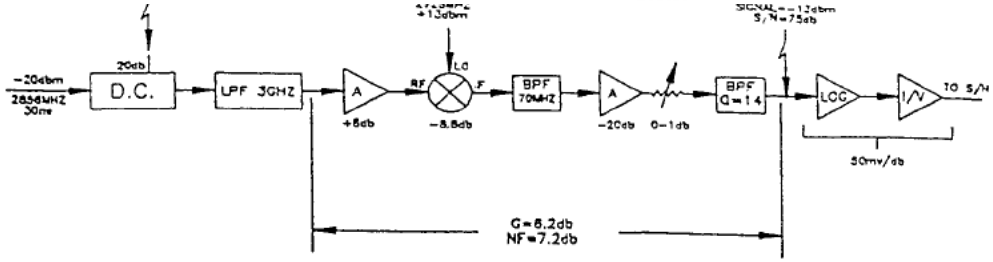

Fig. 3. BPM signal processing electronics

Conventional heterodyne technique with a fundamental 2856 MHz for e- and e+ 30-ns pulsed beams for a stripline bpm

1. Referred by R. Fuja and Y. Chung, "APS linac beam position monitors and electronics"
2. The linac commissioning began in early October of 1993.

It is difficult to separately detect both e- and e+ bunch characteristics.

Choice from the viewpoint on the pros and cons for detection techniques

To the best of my knowledge in 2018,

1. ***Based on the detection technique in time domain,***
   - ✓ **Any high frequency signal losses for all *rf* components, transmission lines and signal pickups should be fully corrected in sufficient wide bandwidth.**
   - ✓ **Is such a correction scheme possible in time domain?**
   - ✓ **How much bandwidth is required at minimum?**
   - ✓ **This technique gives a great advantage in comparison with that in frequency domain?**

2. ***Based on the detection technique in frequency domain,***
   - ✓ **any fundamental frequency is not a characteristic frequency for a single bunch,**
   - ✓ **and a heterodyne technique is not so advantageous for a single bunch in comparison with a pulsed beam,**
   - ✓ **and it is difficult to separately detect both *e*- and *e*+ bunch characteristics.**

Wideband beam monitor (WBM)

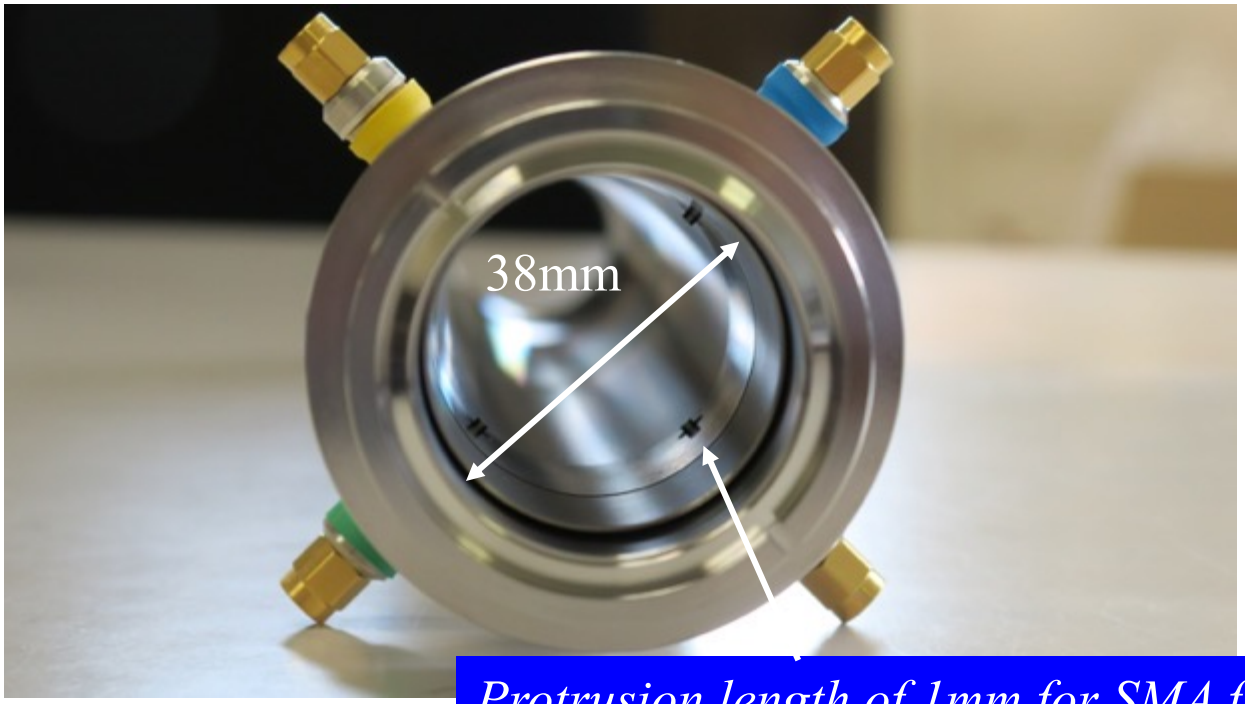

Protrusion length of 1mm for SMA feedthrough antenna from the inner surface

- ✓ *Simultaneous and separate detection for both e- and e+ bunches is possible in time domain with any rf loss corrections for all rf components and transmission lines.*
- ✓ *Fundamental bunch characteristics, bunch interval, charges, transverse positions, and bunch lengths can be separately measured for both e- and e+ bunches in time domain.*

Integrated WBM and steering magnets in a frame

Dipole magnets and WBM fixed in a frame

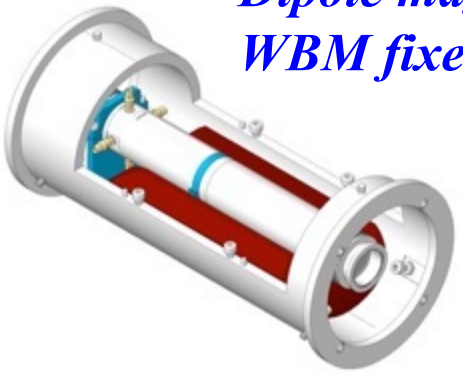

Fixing structure of the frame in a solenoid coil

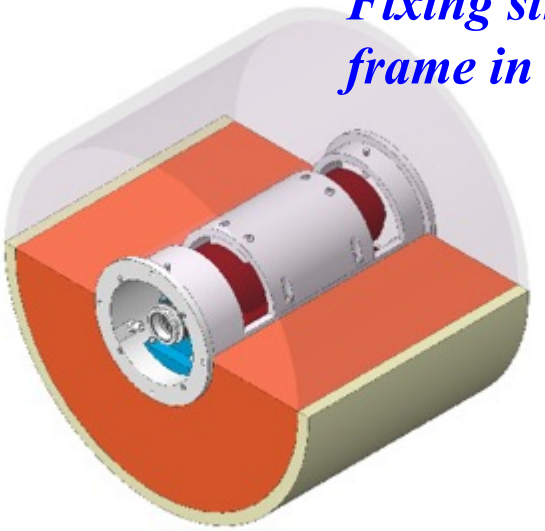

Frame inserted in a solenoid coil

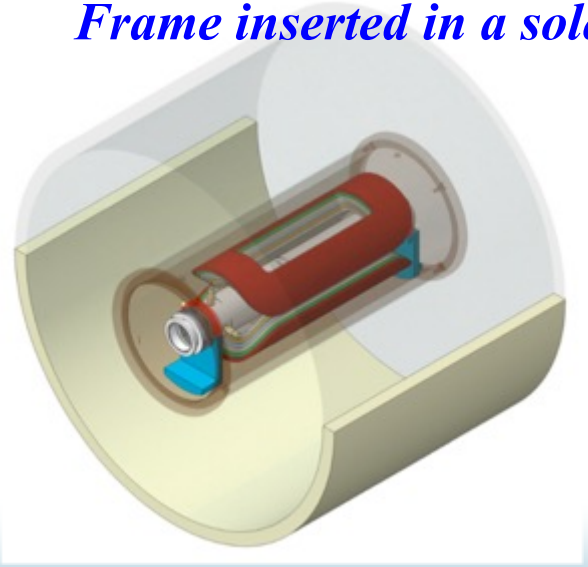

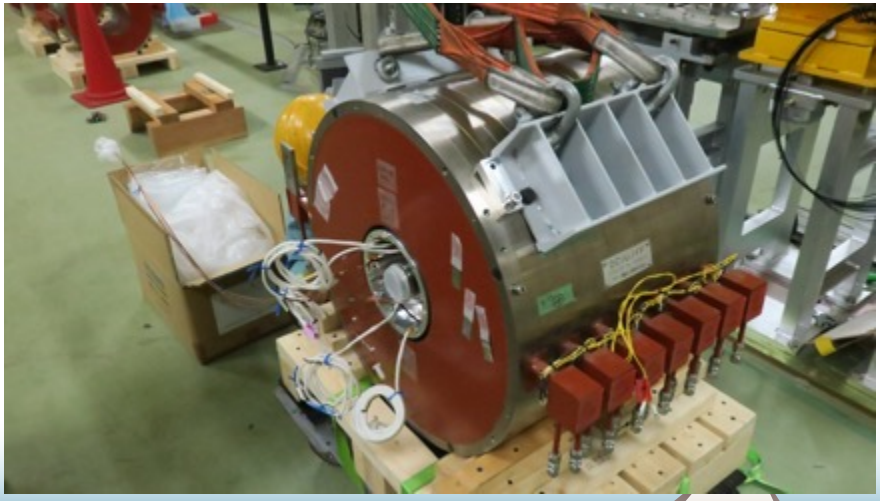

Signal detection system

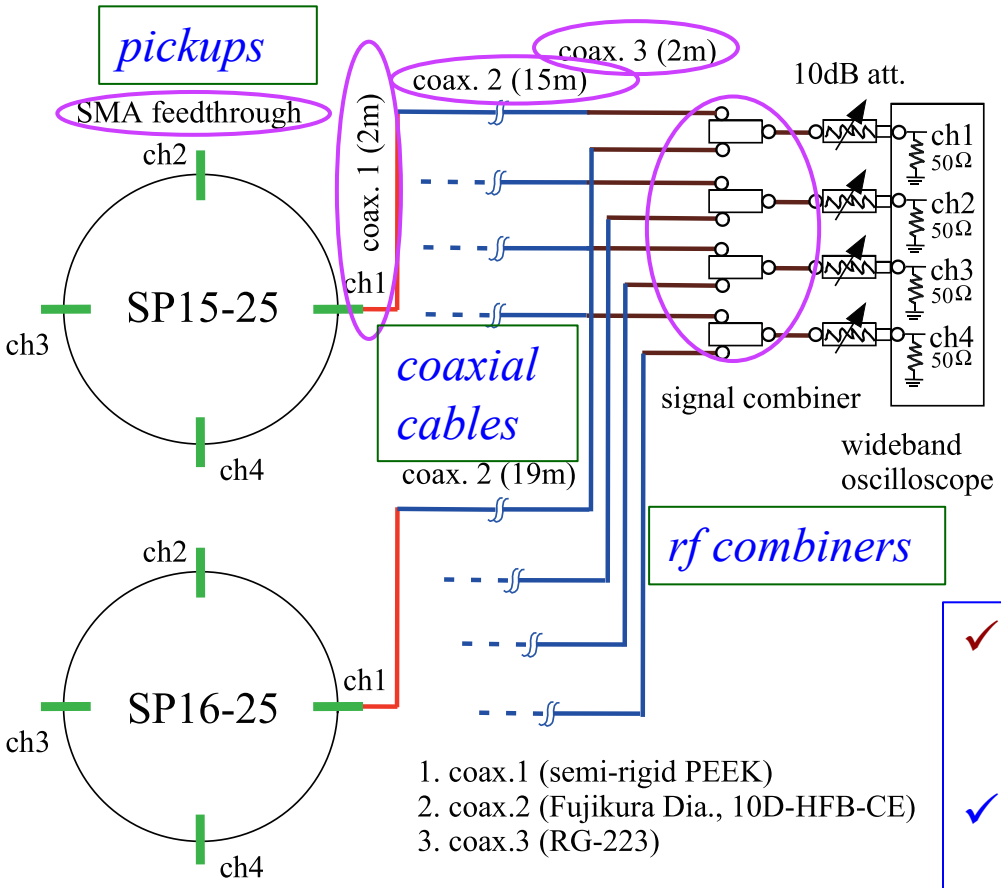

All rf components should be corrected in suitable frequency region by using a vector network analyzer.

- ✓ Coax. cables, *rf* combiners, and *rf loss* in pickups

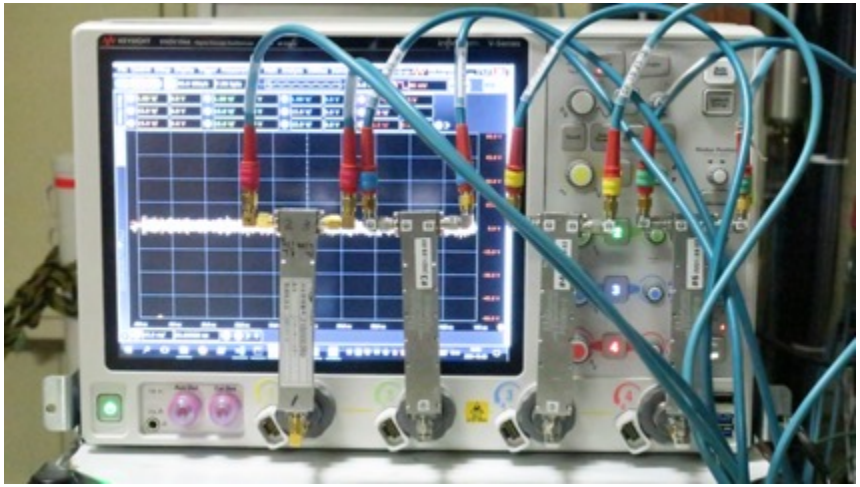

Wideband oscilloscope

- ✓ Keysight Tech., BW13.5GHz, 40GSa/s.

- ✓ *Any rf signal loss corrections are available with normal and inverse FFT procedures based on "de-embedding technique".*
- ✓ *The cut-off frequency was fixed to 9.1 GHz in the inverse FFT procedure.*
- ✓ *Any signal waveforms can be corrected in frequency domain and displayed pulse-by-pulse in time domain.*

Results of the signal detection in time domain

Raw signal

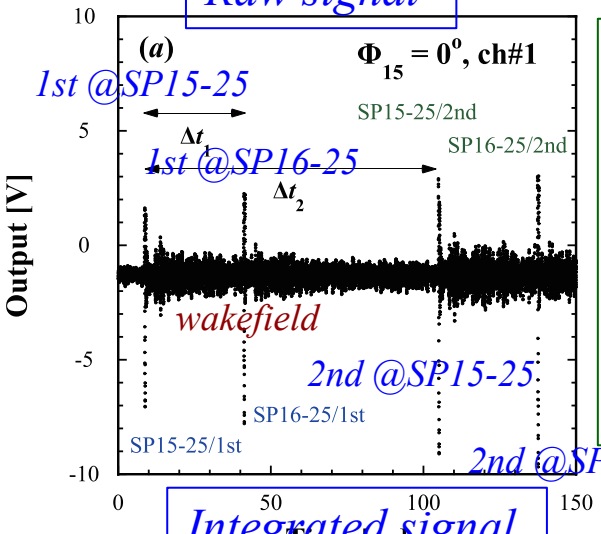

Raw signal (ch#1)

1) *with rf-loss correction,*
2) at ϕ_15=0 deg *in nominal e+ operation,*
3) 2 WBM signals combined,
4) 2 bunch acceleration with the time interval of Δt_2=96 ns

Differential signal

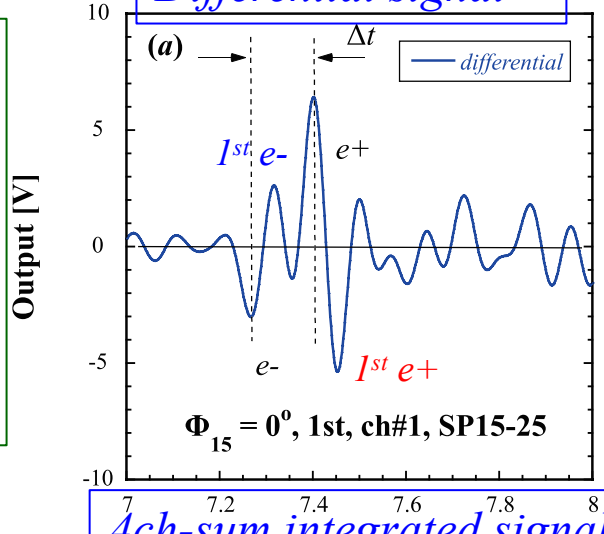

Integrated signal

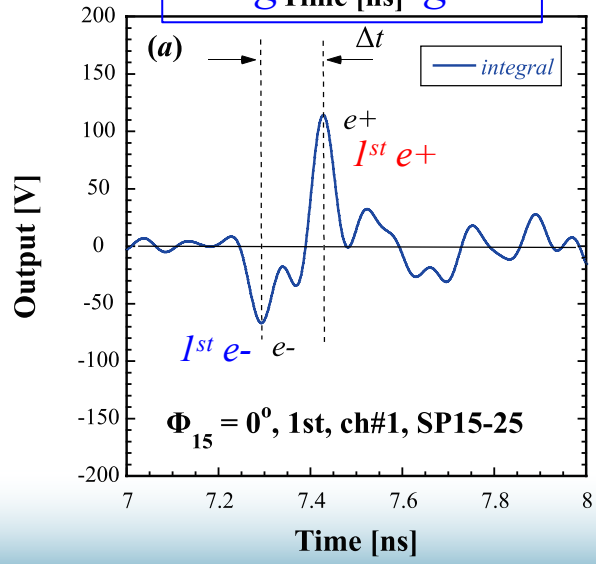

Integrated signal
for beam position calculation,
4ch-sum Integrated signal
for bunch length (pulse width), arrival timing (peak timing), and bunch charge (pulse area) calculation.

4ch-sum integrated signal

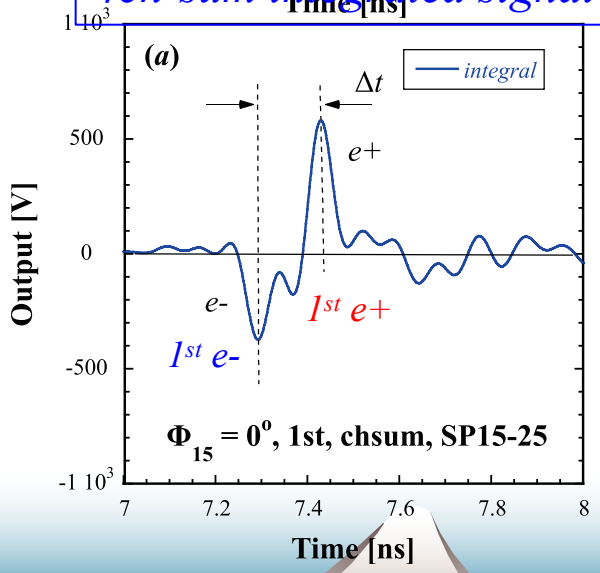

Variations during the dynamical phase-slip process for both the e+e- bunches depending on the capture phase

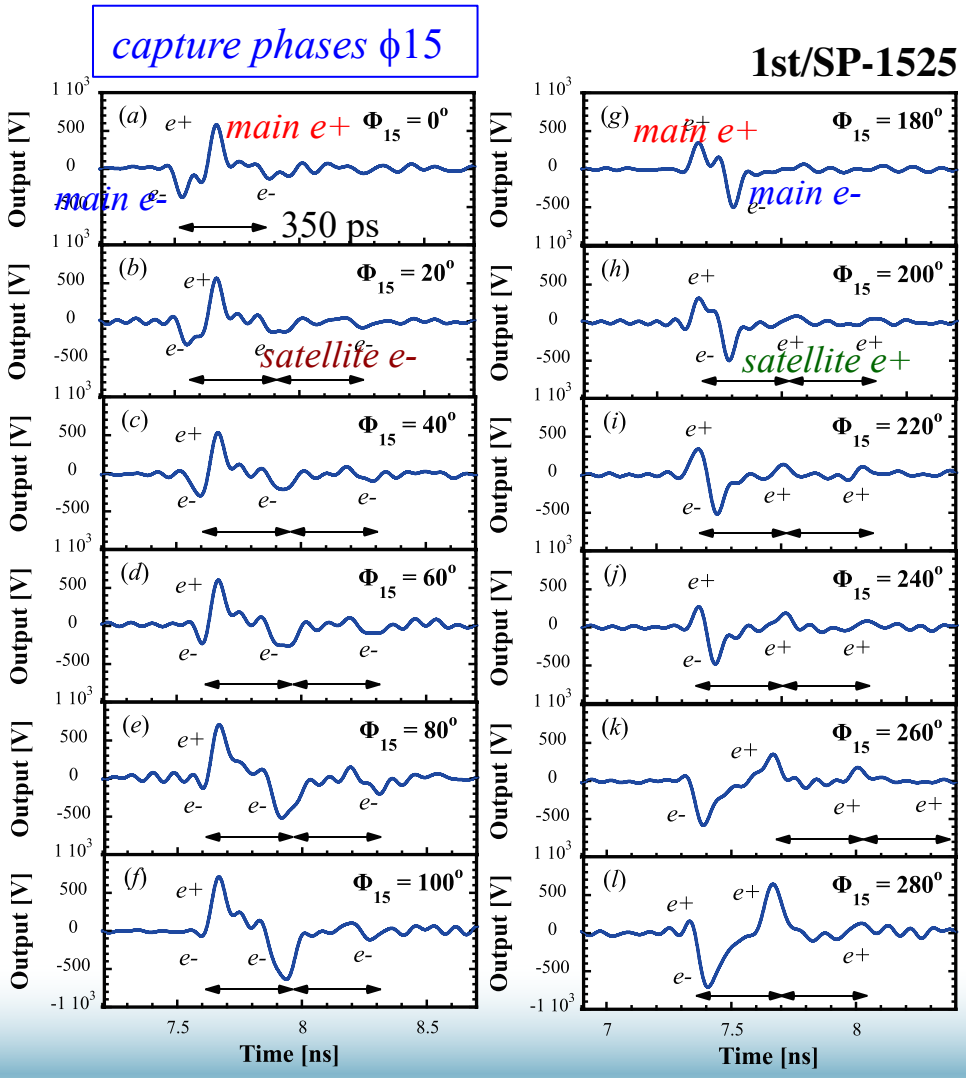

(1) The separate detection for *e-e+* bunches in time domain was successfully performed.
(2) The travelling order of *e-e+* bunches is reversed at certain capture phases through the dynamical phase-slip process.
(3) Some satellite bunches can be identified which are 350ps apart from the main bunch. The generation of satellite bunches is caused by spill-over from the longitudinal phase space.
(4) The results show that quite symmetric dynamical behaviors for both the bunch characteristics were observed.
(5) The ringing waves following from the bunch signals are due to wakefields from upstream accelerator structures.

Time interval measurements as a function of the capture phase

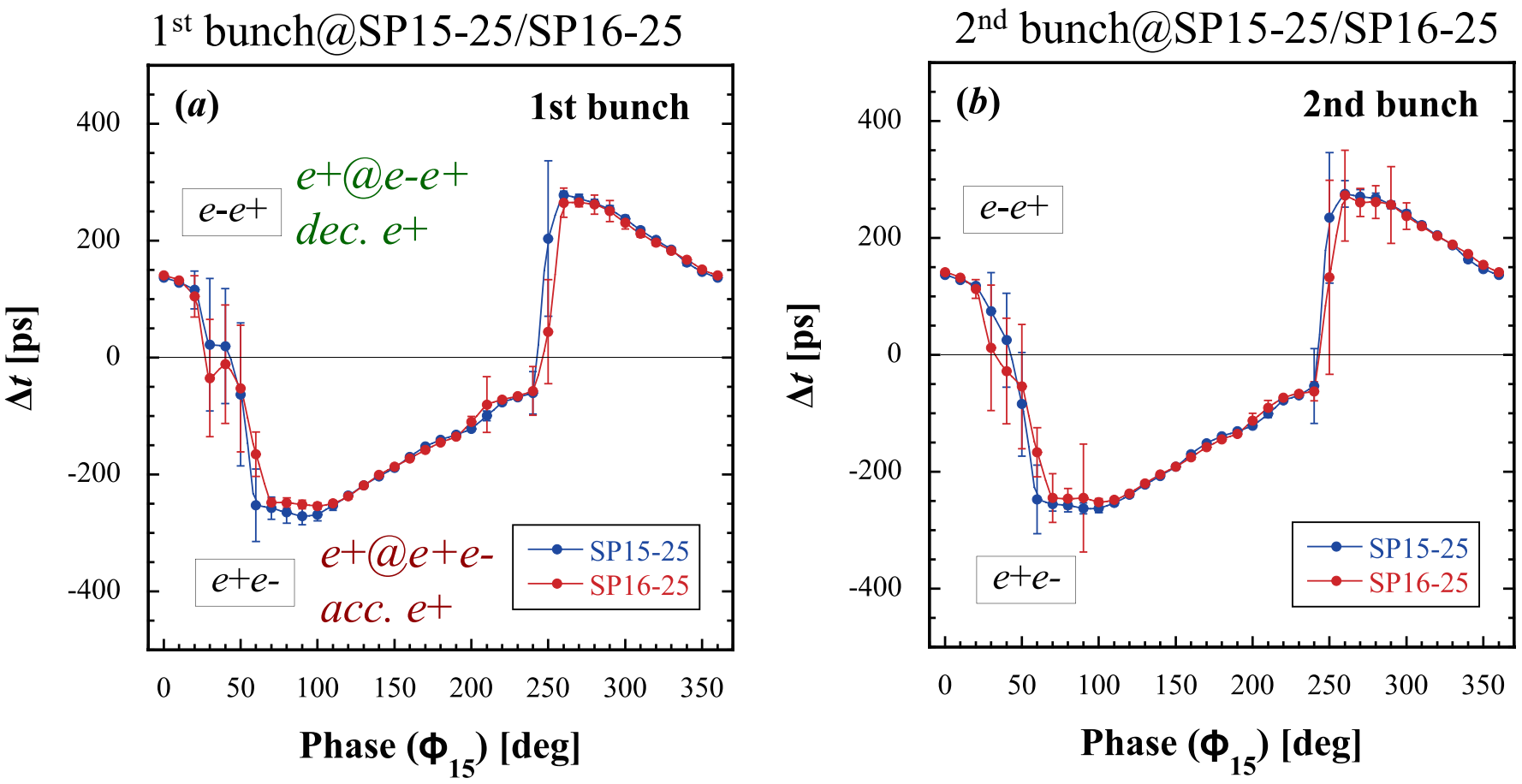

Tsuyoshi Suwada, "Direct Observation of Positron Capture Process at the Positron Source of the SuperKEKB B-Factory"; *Scientific Reports* **12,** 18554 (2022). Published online 2022 Nov. 03. https://doi.org/10.1038/s41598-022-22030-5.

3D plots in the bunch characteristics as functions of time interval, capture phase, and bunch intensity for e+e- bunches

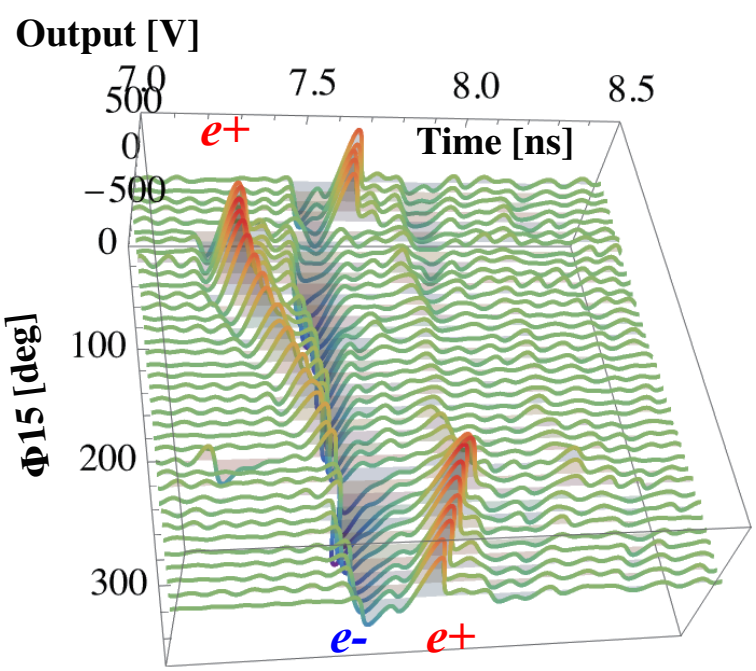

(*a*) 1st bunch, SP15-25

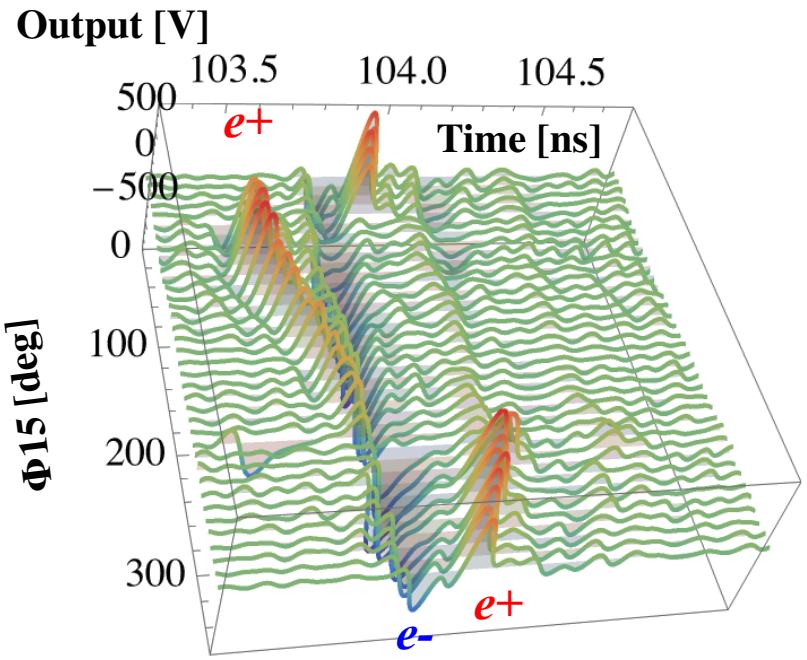

(*b*) 2nd bunch, SP15-25

1st bunch@SP15-25/SP16-25

2nd bunch@SP15-25/SP16-25

e+e- bunch characteristics depending on the capture phase

e- decelerating region *e- accelerating region* *e+ accelerating region* *e+ decelerating region*

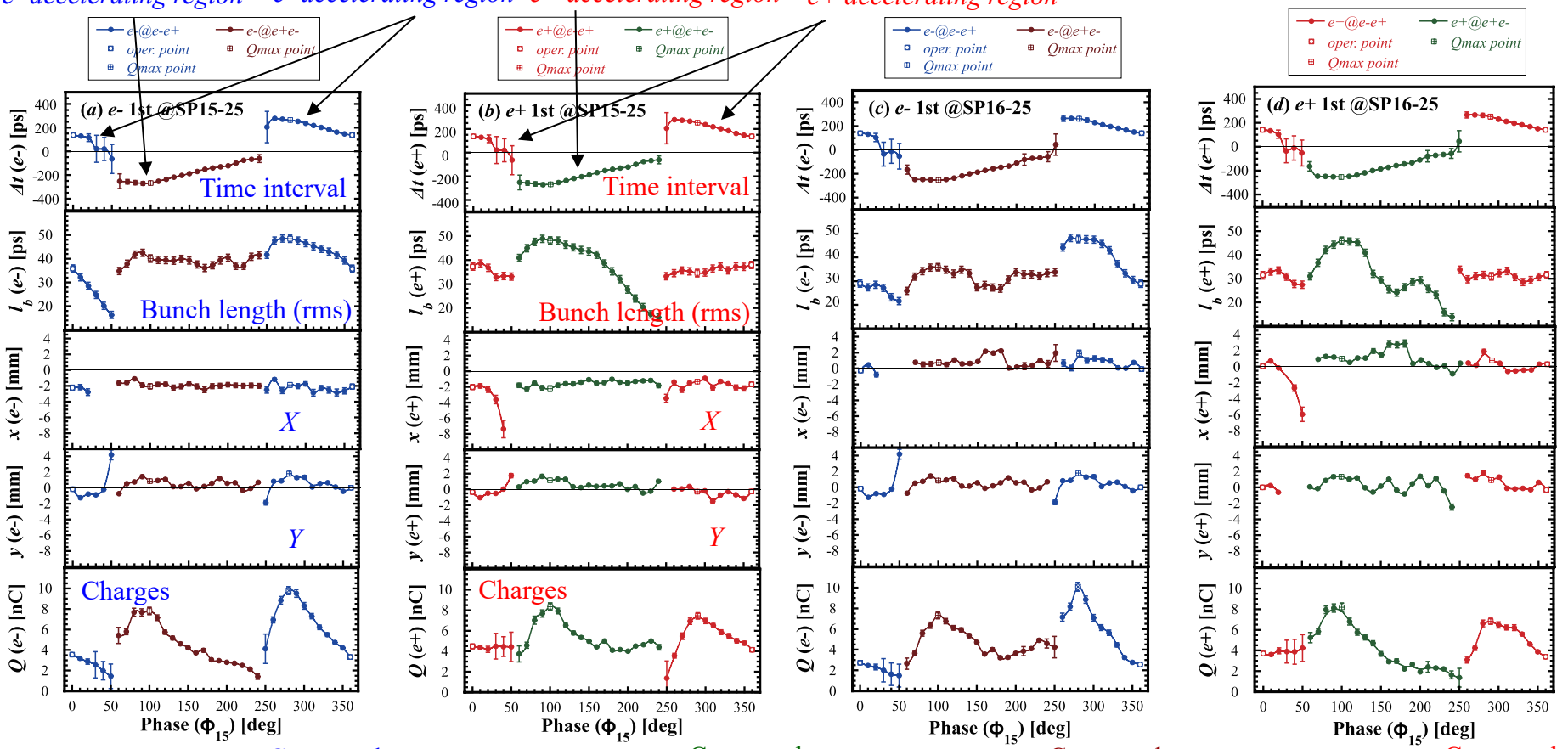

Capture phase

1st e-@e-e+,
1st e-@e+e- at SP15-25,
Step phase Δϕ15=Δϕ16=10°

Capture phase

1st e+@e-e+,
1st e+@e+e- at SP15-25

Capture phase

1st e-@e-e+,
1st e-@e+e- at SP16-25

Capture phase

1st e+@e-e+,
1st e+@e+e- at SP16-25

Plots for both the e+e- bunch positions at SP15-25 and SP16-25

1st e-

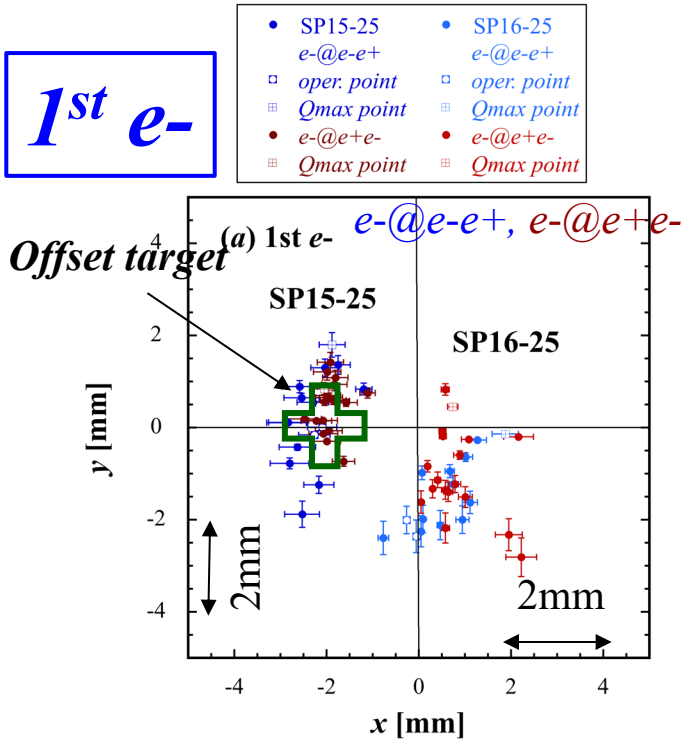

1st e+

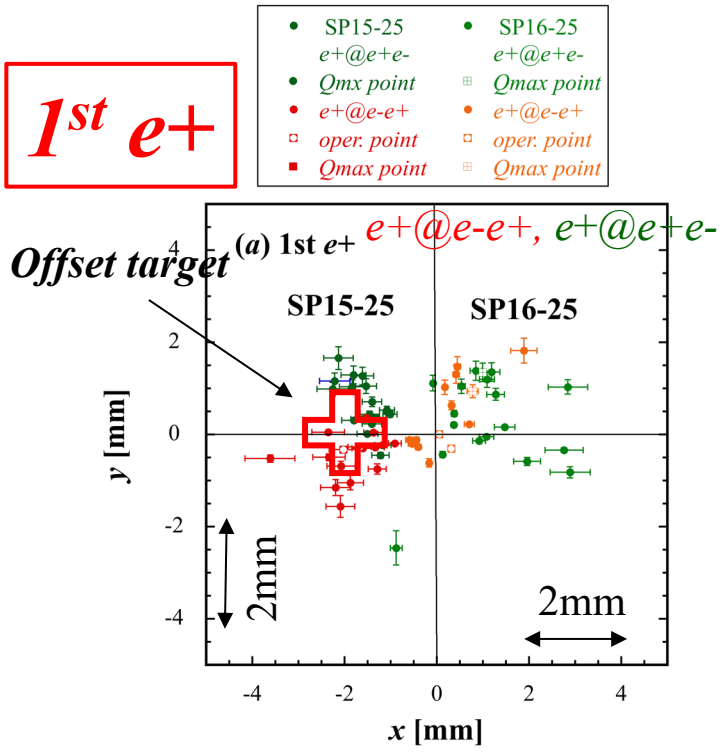

- It can be found that there are no characteristic differences in the transverse positions depending on the capture phase under the nominal operation condition and those giving the maximum charges.
- It is interesting that the cluster for each bunch rotates in the transverse plane owing to their cyclotron motion in the longitudinal direction between SP15-25 and SP16-25.

Correlation plots for the time interval and bunch charges of both e+e- bunches at SP15-25 and SP16-25

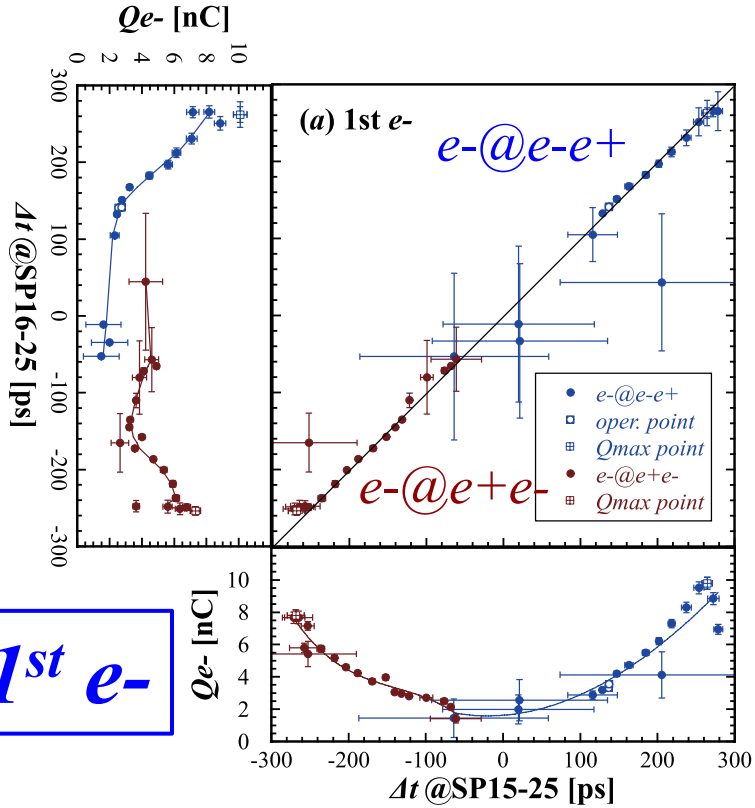

1st e-

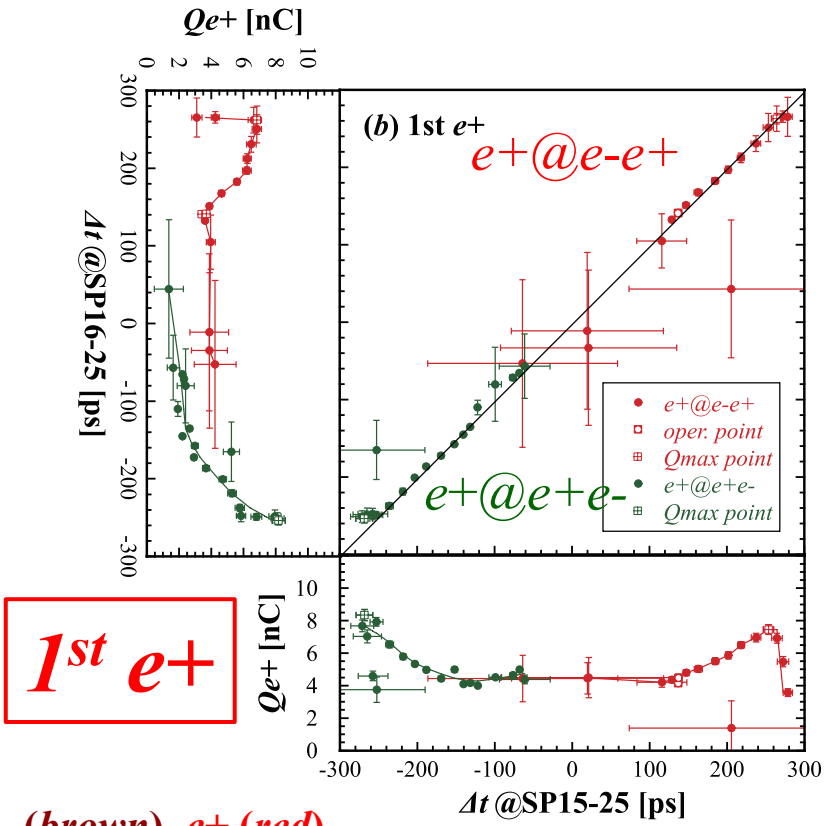

1st e+

Accelerating e- (blue), e+ (green), decelerating e- (brown), e+ (red)

- *The time interval correlation is based on a 45º inclined line.*
- *This result means that the dynamical phase slip process was completed at the first WBM (SP15-25).*
- *The maximum charges are generated at the maximum time intervals even for the different bunches,*

Δt~-268 ps (*Δt*~-268 ps)@ *acc. e- (acc. e+), Δt*~-264 ps (*Δt*~253 ps)@ *dec. e- (dec. e+), respectively.*

Correlation plots for the bunch length and bunch charges of both e+e- bunches at SP15-25 and SP16-25

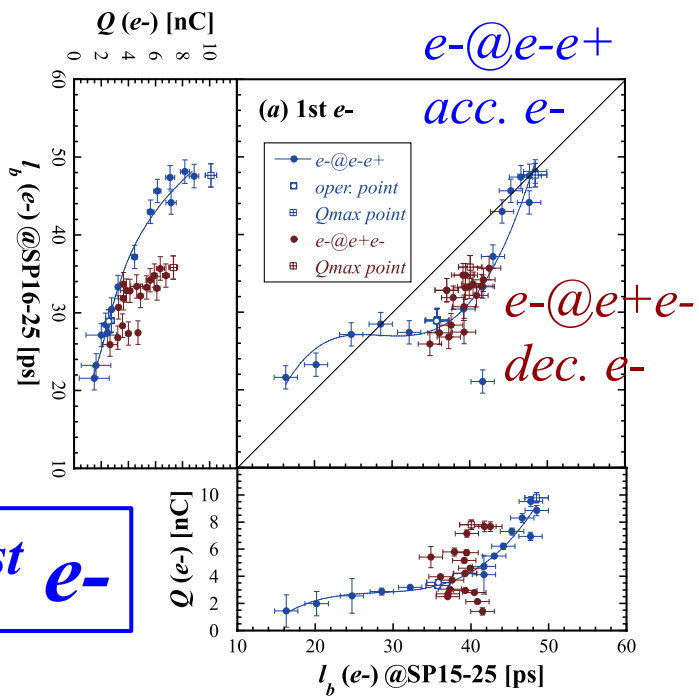

1st e-

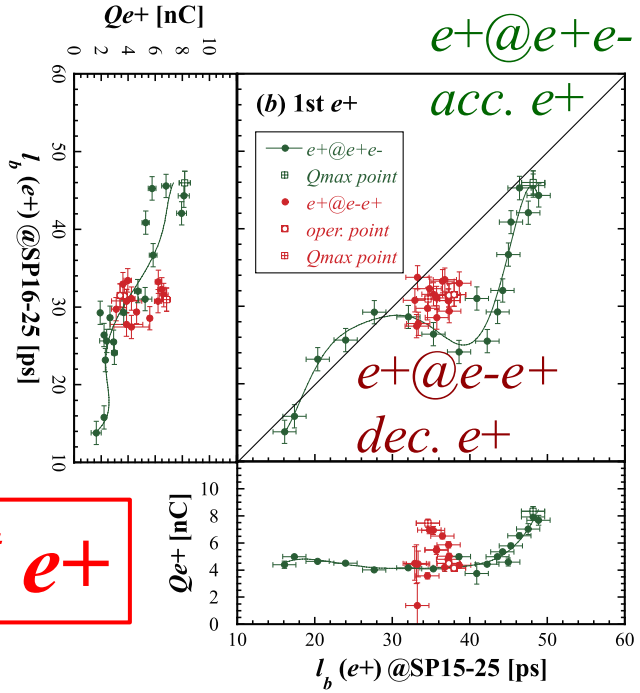

1st e+

- *Although the dynamical phase-slip process was fixed at the front WBM (SP15-25), the dynamical exchange of particles in the longitudinal direction inside the bunch may be caused, called bunch lengthening (or shortening).*
- *The correlation seems to be based on a 3rd-order polynomial function in the accelerating phase region, and on the other hand, that shows a bunch shortening in the decelerating phase region.*
- *The maximum bunch charges are generated at the maximum bunch length.*

Variations in e+e- bunch charges as a function of the capture phase at SP15-25 and SP16-25

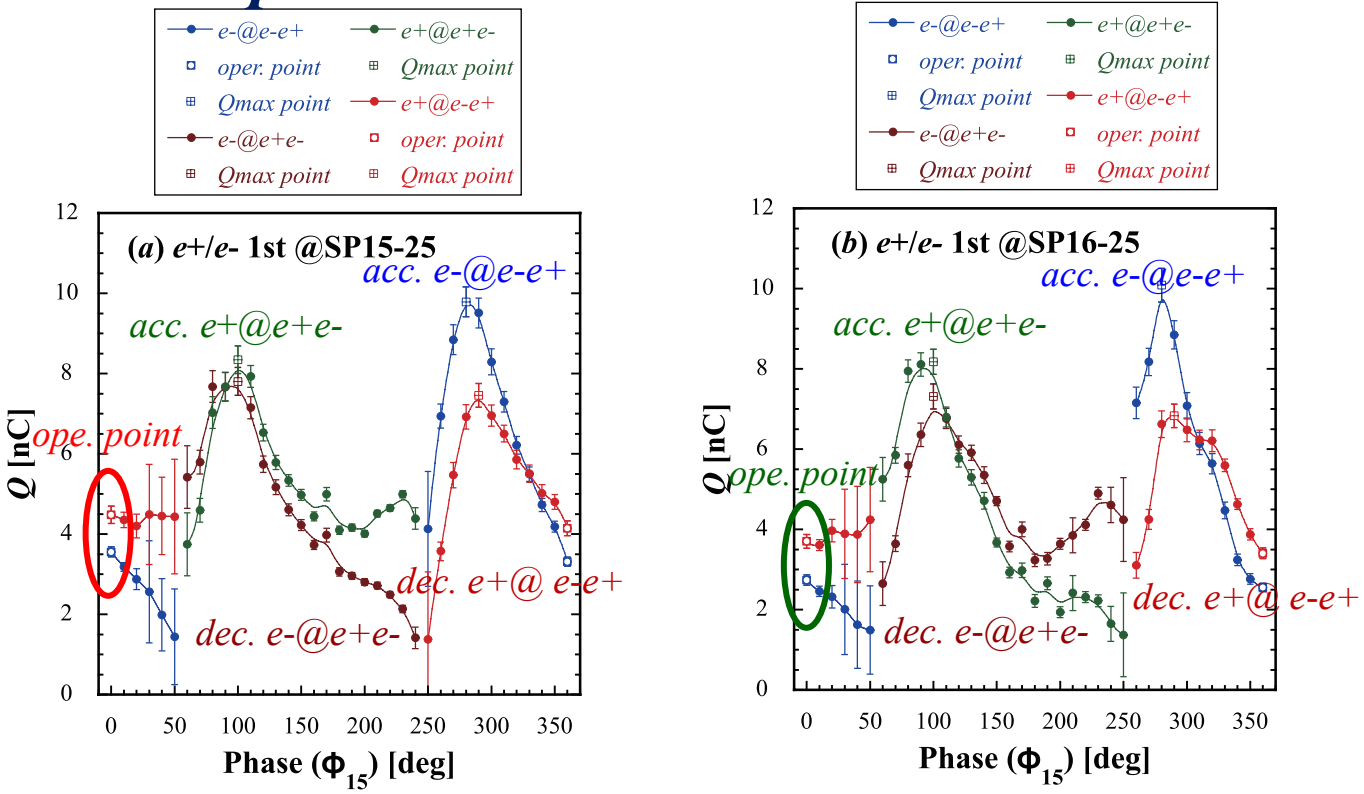

- *The present operation point is not on an optimized point.*
- *The e+e- bunch charges in the accelerating phase region are greater than those in the decelerating phase region in the capture section.*
- *The e+ yields at the peak points in the acc. and dec. phase regions are 122% and 84% greater than that at the nominal operation point, respectively.*

Conclusions

- Direct simultaneous measurements of the secondary e+e- bunch characteristics were successfully performed with WBMs at the e+ source of the SuperKEKB B-factory.
- Longitudinal and transverse bunch characteristics were obtained for each bunch as a function of the capture phase to investigate their dynamical capture process under two-bunch acceleration scheme.
- The results show that quite symmetric behaviors in the e−e+ bunch characteristics were observed.
- Such wideband detection techniques could be applied to conventional and advanced e+ sources in future accelerator projects.
- Based on this technique, the e+ intensity could be systematically optimized in multidimensional parameter spaces towards high-intensity e+ sources.

Backup files

Variations in the e+ bunch charges as a function of the capture phase at SP15-25, SP16-25, and SP16-5

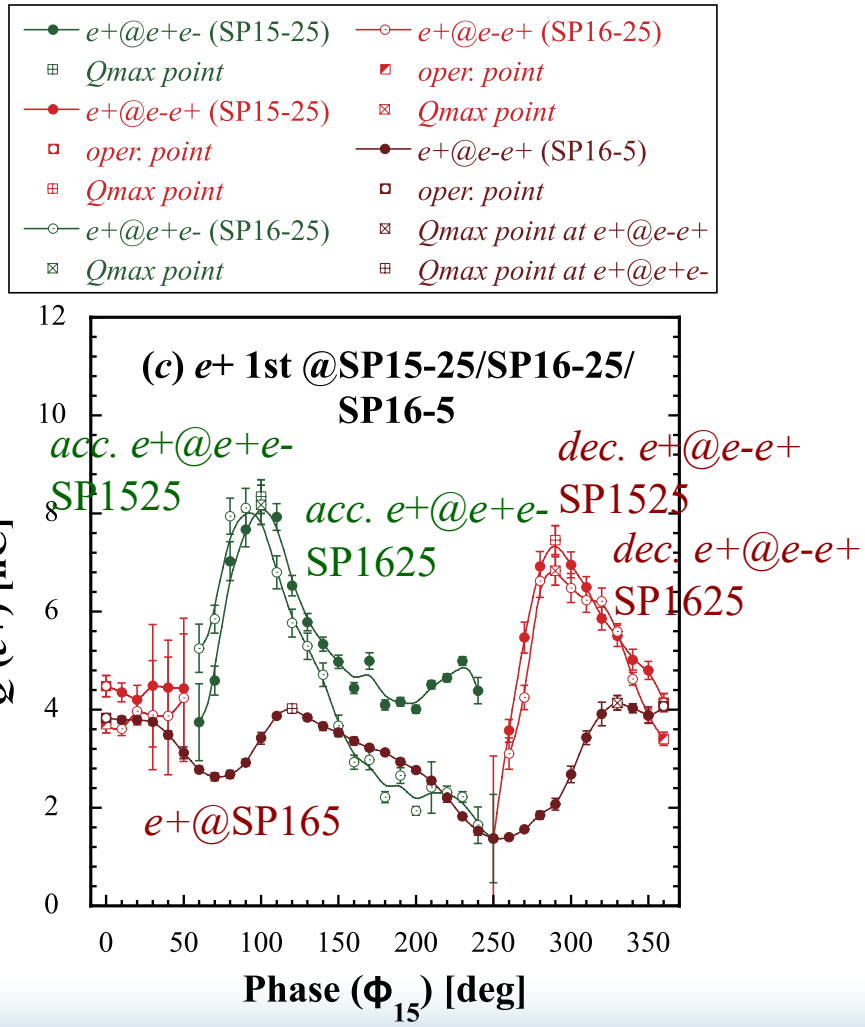

- *It is clear that the present operation point is not on an optimized point.*
- *The e+ yield at the maximum point obtained by a BPM after the capture section is only ~5% greater than that at the nominal operation point.*
- *The capture phase at the max. e+ yield in the capture section is shifted from that after the capture section.*
- *The results show that only the e+ yield measurement at the location after the capture section is not sufficient in the optimization procedure. More detailed parameter tunings may be required.*

Layout of the e+ source of the SKEKB injector linac

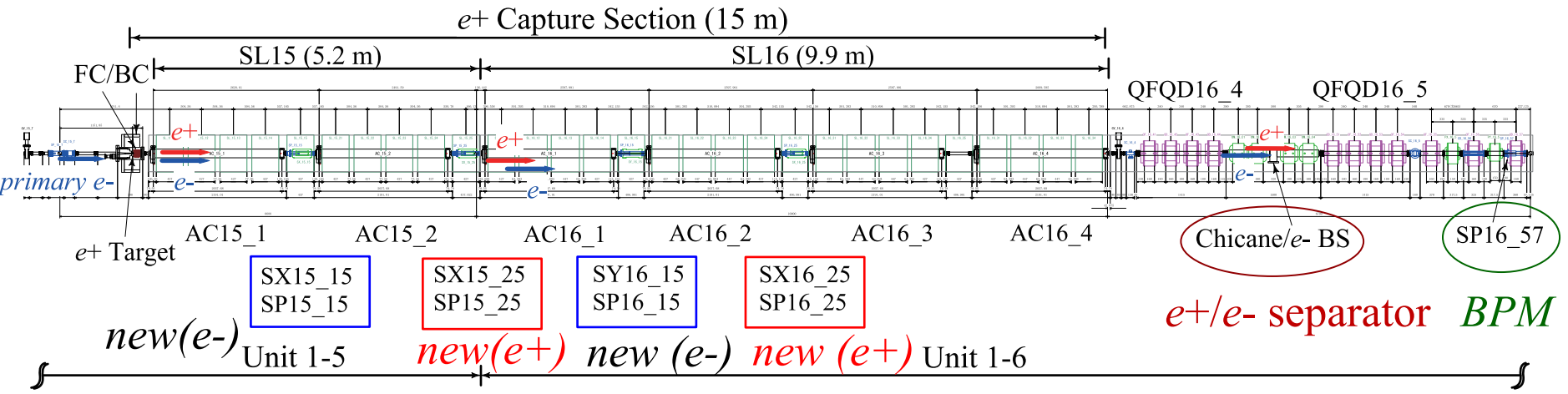

- Total length of the capture section ~15 m
- *Primary Ee-* = 3.5 GeV, ~10 nC (*single-bunch*)
- *Ee+* ~ 120 MeV after the capture section
- *e+ target 14mm-thick W*
- Solenoidal fields of FC/BC 3.5/1.5 T
- Solenoidal fields of DC SLs 0.4 T(unit1-5) /0.5 T(unit1-6)
- LAS Acc. gains 14-20 MV/m (unit1-5) / 10 MV/m (unit1-6)
- Wideband monitors (*new for e+*) and conventional BPMs (*new for e-*)

The SuperKEKB B-Factory: an electron-positron collider with asymmetric energies

Upgraded components for SuperKEKB

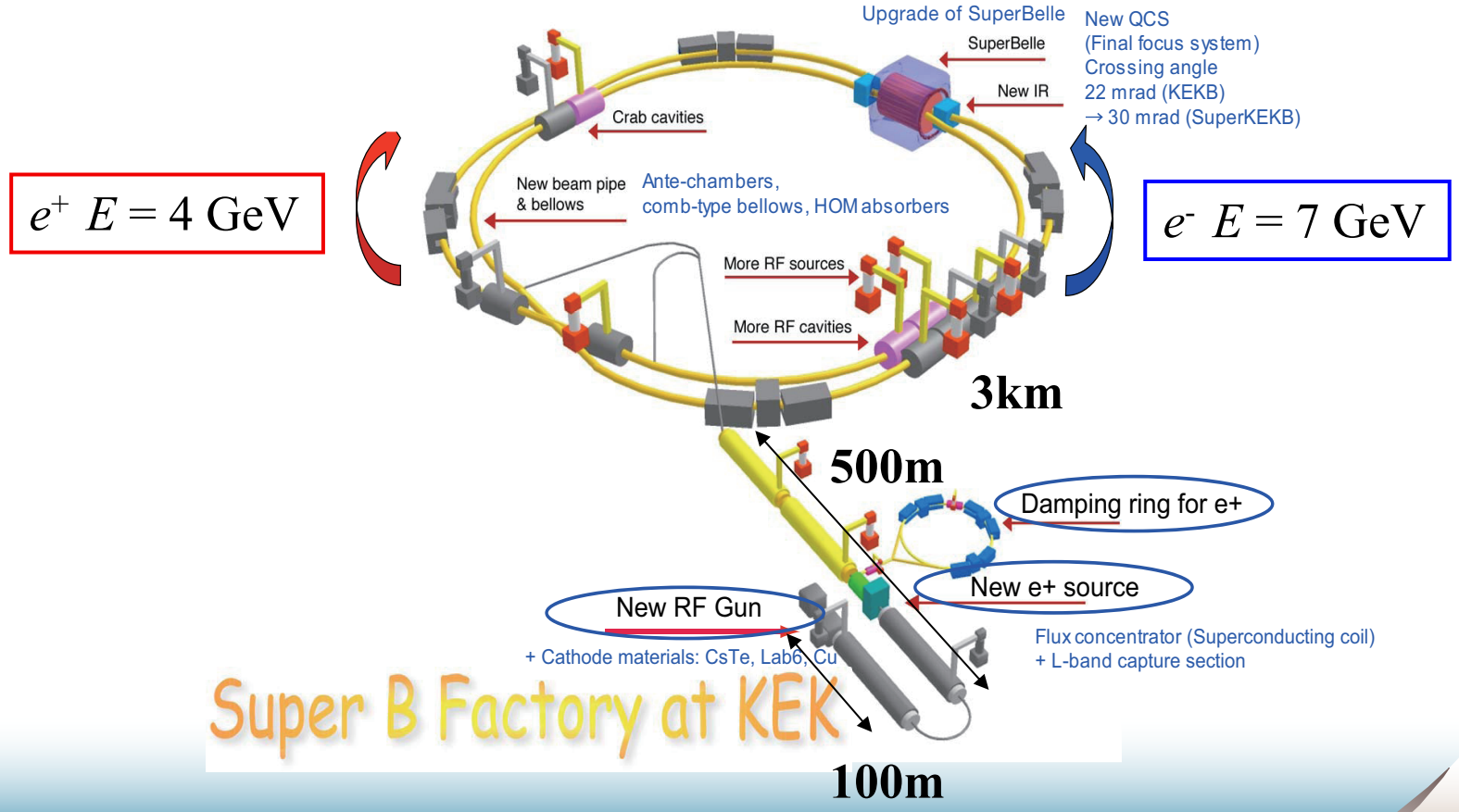

References

1. Tsuyoshi Suwada, Muhammad Abdul Rehman, and Fusashi Miyahara, “First simultaneous detection of electron and positron bunches at the positron capture section of the SuperKEKB factory”; *Scientific Reports* **11,** 12751 (2021). https://doi.org/10.1038/s41598-021-91707-0.
2. Tsuyoshi Suwada, “Modal Analysis of Electromagnetic Couplings between SMA-Feedthrough Electrode and Beam for Wideband Beam Monitor”; Poster presented at *the 10th International Beam Instrumentation Conference (IBIC2021)*, *Video meeting hosted by PAL, Korea*, Sep. 13-16, 2021, pp. 392-395 (JACoW Publishing, 2021) [ISBN 978-3-95450-230-1, doi:10.18429/JACoW-IBIC2021-WEPP12].
3. M. A. Rehman and T. Suwada, “Observation of Wakefireld Effects with Wideband Feedthrough-BPM at the Positron Capture Section of the SuperKEKB Injector Linac”; *Proceedings of the 10th International Beam Instrumentation Conference (IBIC2021)*, Pohang, Rep. of Korea, Sep. 13-16, 2021, pp. 52-55 (JACoW Publishing, 2021) [ISBN 978-3-95450-230-1, doi:10.18429/JACoW-IBIC2021-MOPP10].
4. M.A. Rehman, T. Suwada, and M. Miyahara; “First synchronous measurement of single-bunched electron and positron beams with a wideband feedthrough-BPM at the positron capture section of the SuperKEKB inejctor linac”; *Proceedings of the 2021 Particle Accelerator Conference* (*IPAC’21*), hosted by the Brazilian Center for Research in Energy and Materials (CNPEM), Campinas, Brazil, May 24-28, 2021, pp.557-560 (MOPAB163); ISBN: 978-3-95450-214-1, ISSN: 2673-5490, doi:10.18429/JACoW-IPAC2021-MOPAB163.
5. T. Suwada, “Characteristic Analysis of Wideband Beam Monitor with High Frequency Pickups”; Rev. Sci. Instrum. **93,** 093301 (2022) [DOI: 10.1063/5.0087321].
6. Tsuyoshi Suwada, “Direct Observation of Positron Capture Process at the Positron Source of the SuperKEKB B-Factory”; *Scientific Reports* **12,** 18554 (2022). Published online 2022 Nov. 03. https://doi.org/10.1038/s41598-022-22030-5.
7. T. Suwada, “First direct measurement of electron and positron bunch characteristics at the positron source of the SuperKEKB B-Factory”; AIP Advances **13**, 045021 (2023); [DOI: 10.1063/5.0145776].

Frequency characteristics for the bunch characteristics

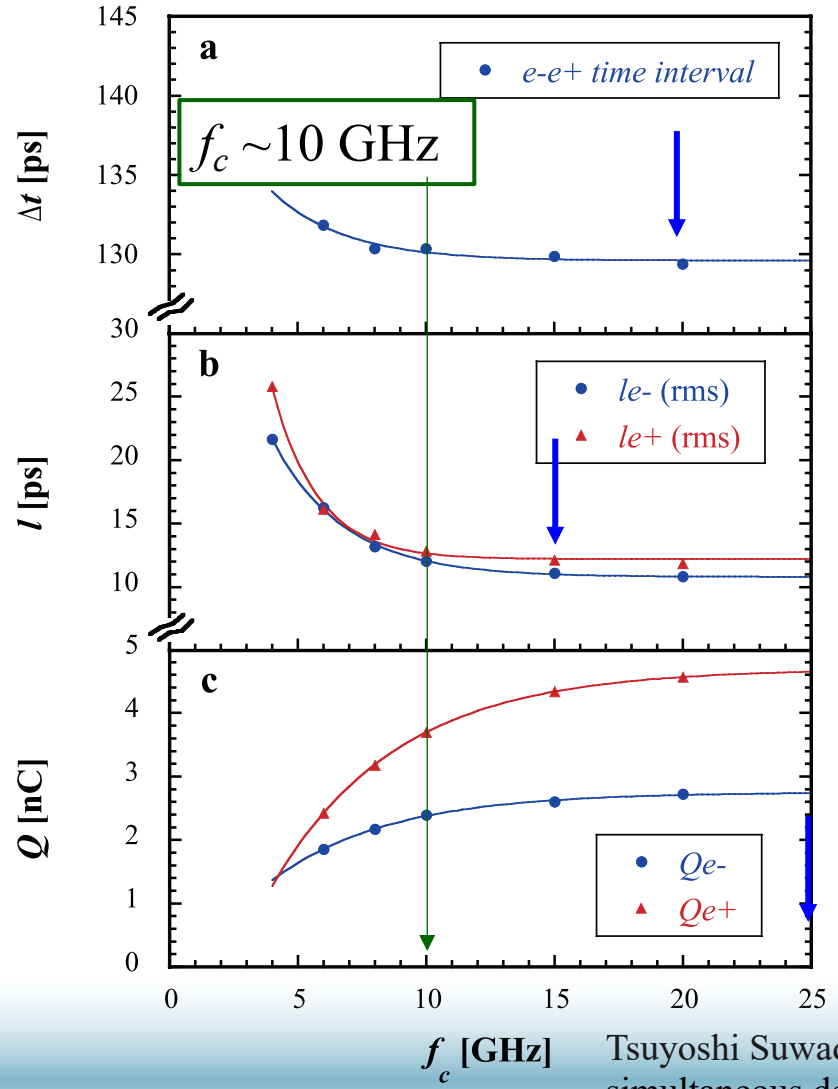

Time interval Δt between e- and e+ bunches, f_c ~10 GHz

systematic error

$\sigma_{\Delta t} = \Delta t$ (20 GHz) - Δt (10 GHz)

Bunch lengths le- and le+

f_c ~10 GHz

systematic error

$\sigma_l = l$ (25 GHz) - l (10 GHz)

Bunch charges Qe- and Qe+

f_c ~20 GHz

systematic error

$\sigma_Q = Q$ (25 GHz) - Q (20 GHz)

Tsuyoshi Suwada, Muhammad Abdul Rehman, and Fusashi Miyahara, "First simultaneous detection of electron and positron bunches at the positron capture section of the SuperKEKB factory"; *Scientific Reports* **11,** 12751 (2021). Published online 2021 June 17. https://doi.org/10.1038/s41598-021-91707-0.

Installation of WPM into a frame

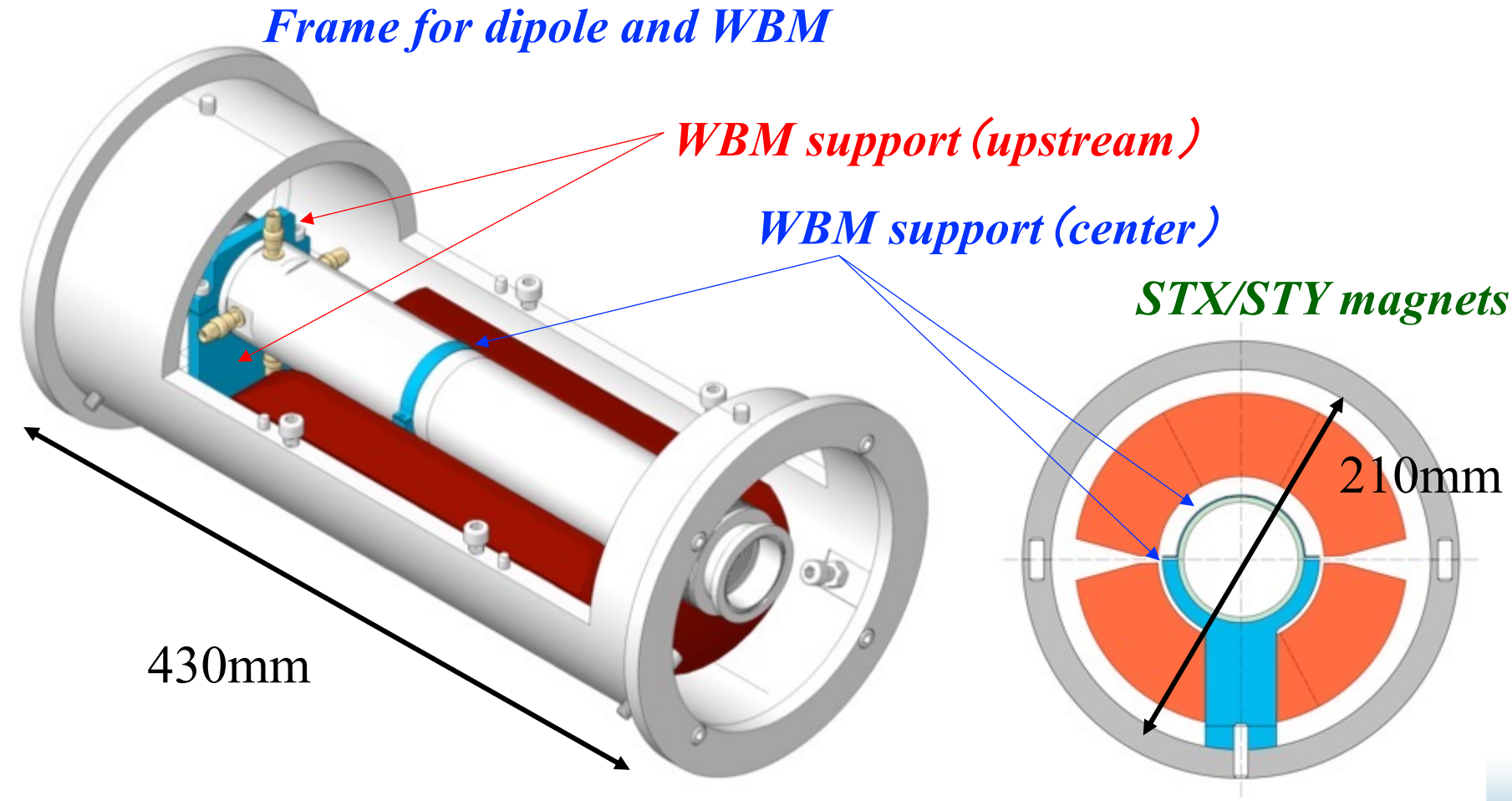

Installation of solenoid coil into the e+ source

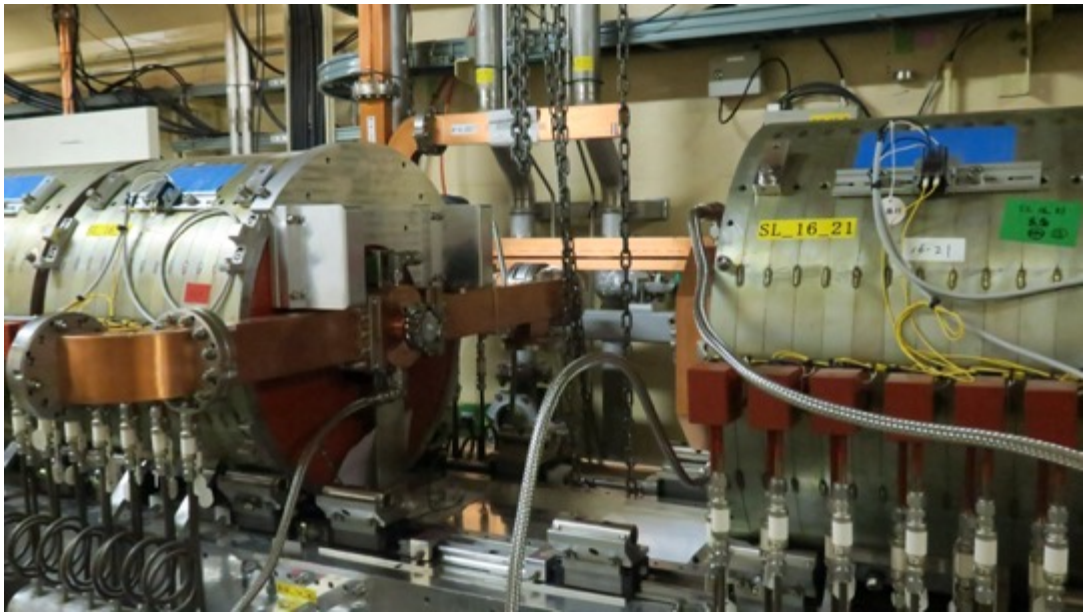

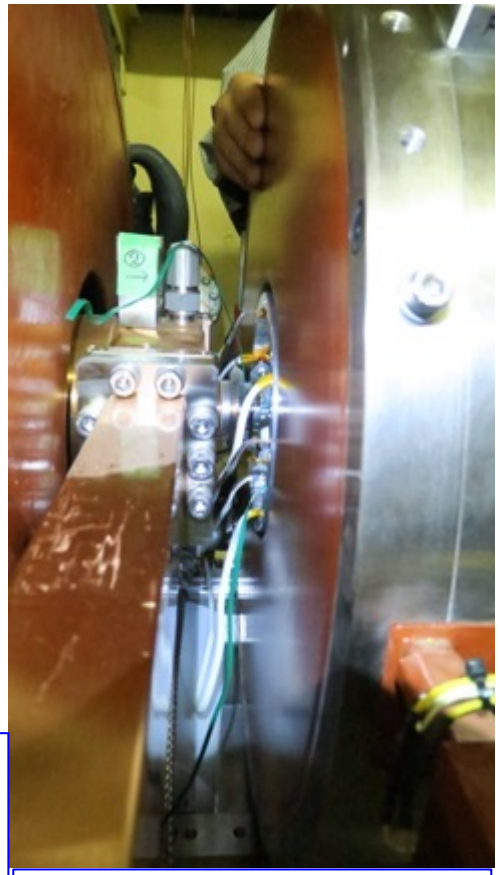

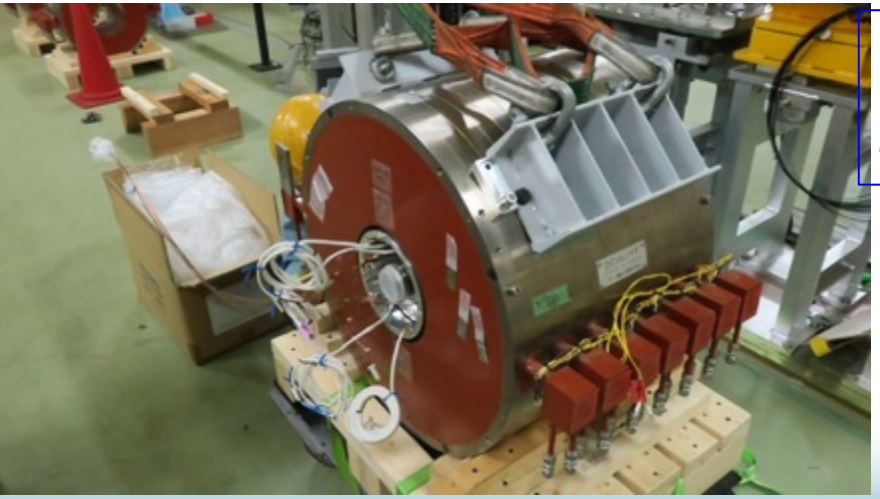

(upper) e+ capture section

Cable extraction

(left) Solenoid coil installed the frame

Dipole magnet and WBM fixed in a frame

Inserting a WBM and dipole magnet in an aluminum frame

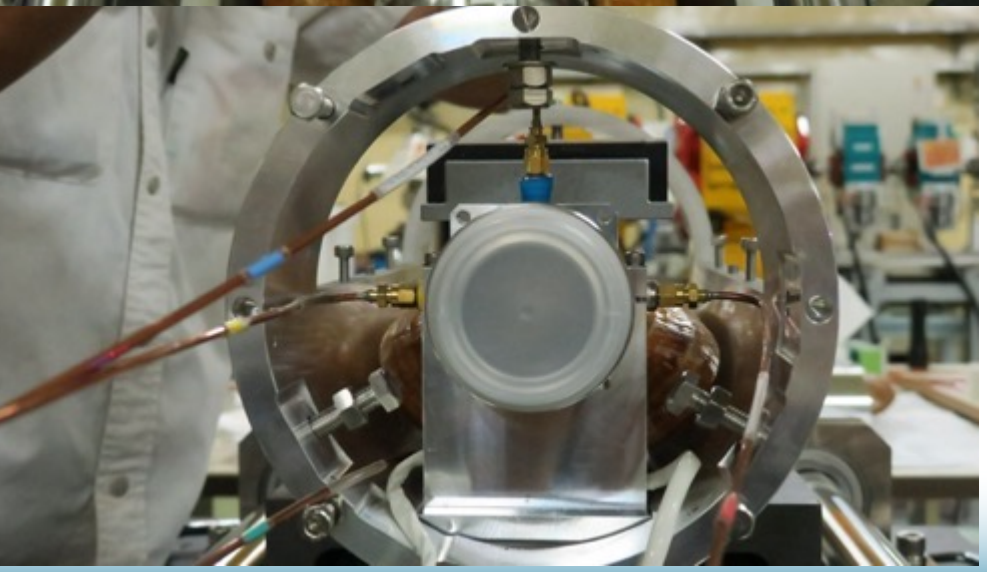

Extracting coax. cables with a bending angle of 90^{o} in the forward direction.

Integrated WBM and semi-rigid coaxial cables filled with PEEK as an insulator

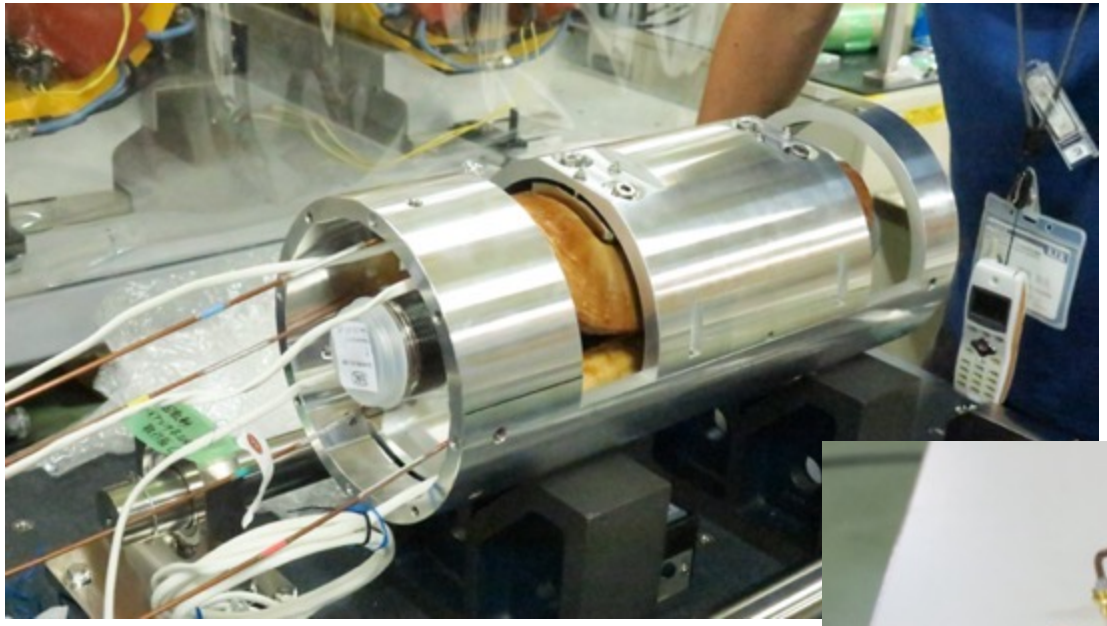

Integrated aluminum frame fixed with WBM and dipole magnet

2m-long signal-extraction coax. cable filled with an insulator made of PEEK

Typical measurement results of there different coax. cables connected in series/amplitude and phase data

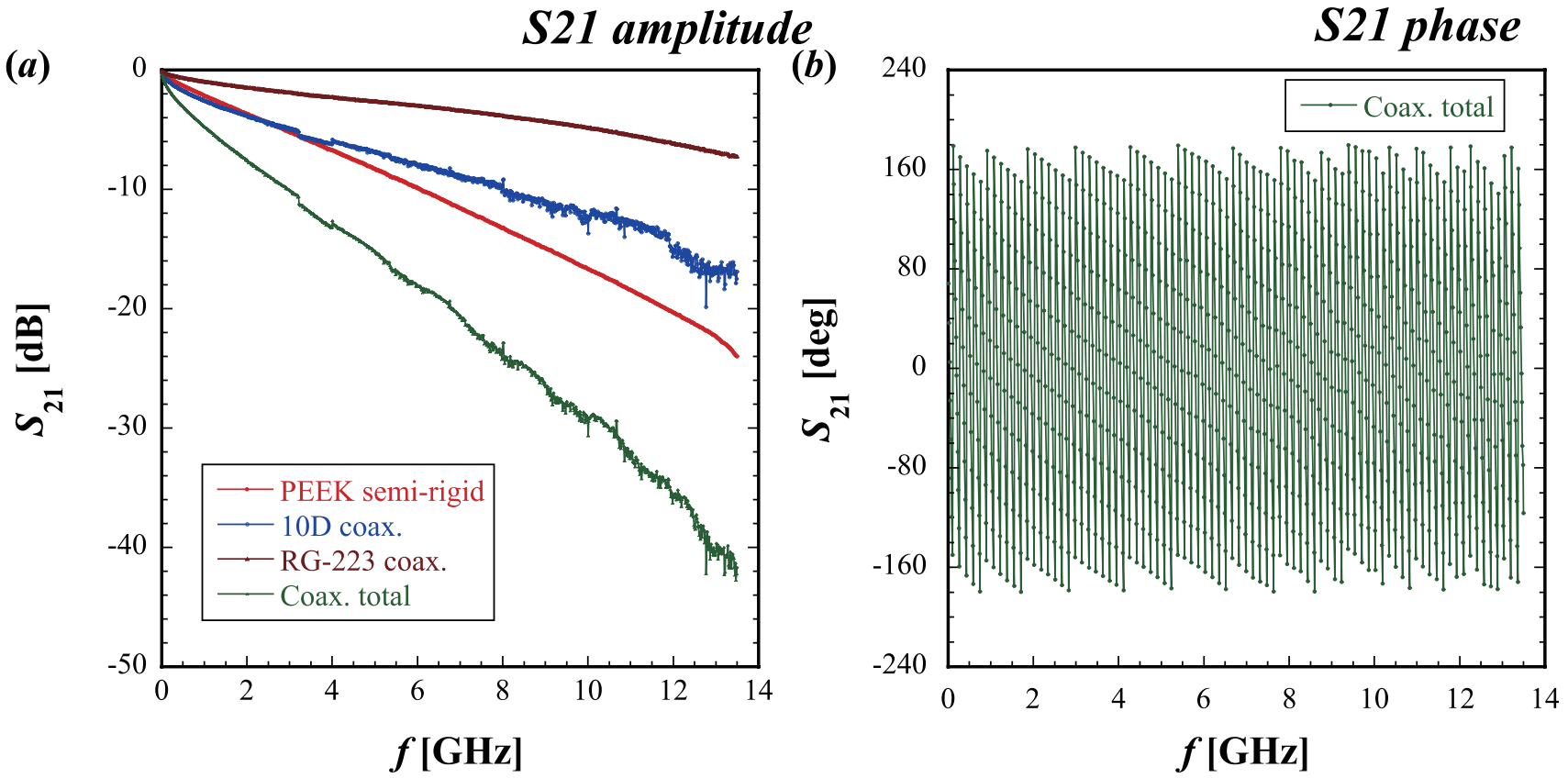

T. Suwada, "Characteristic Analysis of Wideband Beam Monitor with High Frequency Pickups"; Rev. Sci. Instrum. **93,** 093301 (2022) [DOI: 10.1063/5.0087321].

RF loss correction technique for pickups (I)

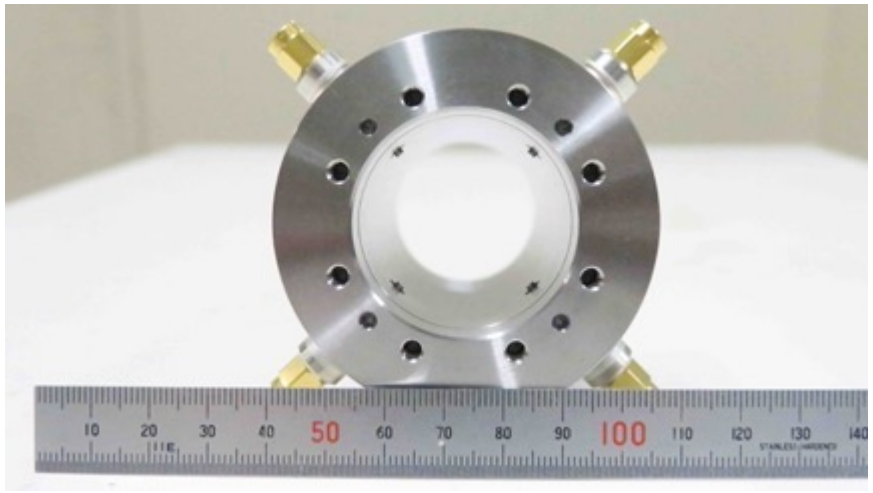

(*a*)

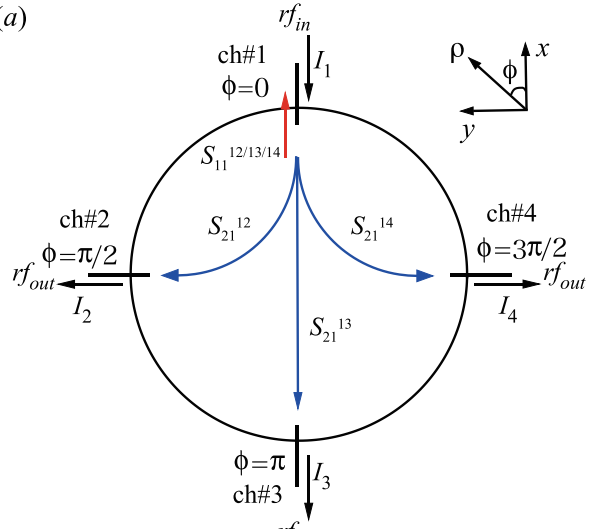

(*b*)

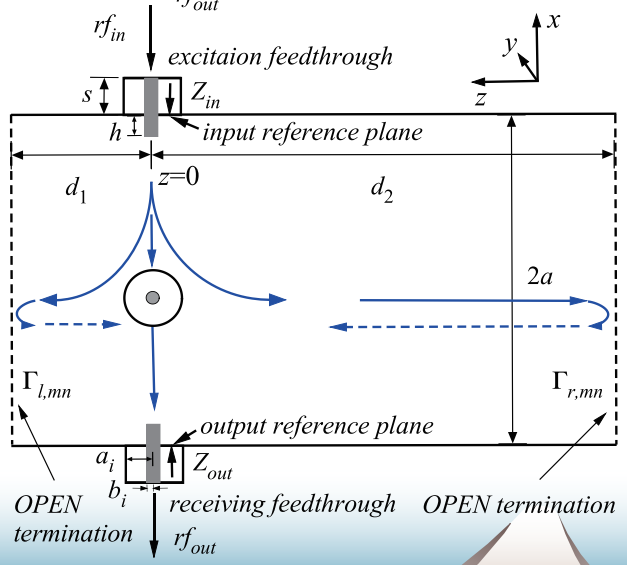

- ✓ *rf induced technique by which S21 between channels is measurable by a VNA*
- ✓ T. Suwada, "*Characteristic Analysis of Wideband Beam Monitor with High Frequency Pickups*"; Rev. Sci. Instrum. **93,** 093301 (2022) [DOI: 10.1063/5.0087321].

RF loss correction technique for pickups (II)

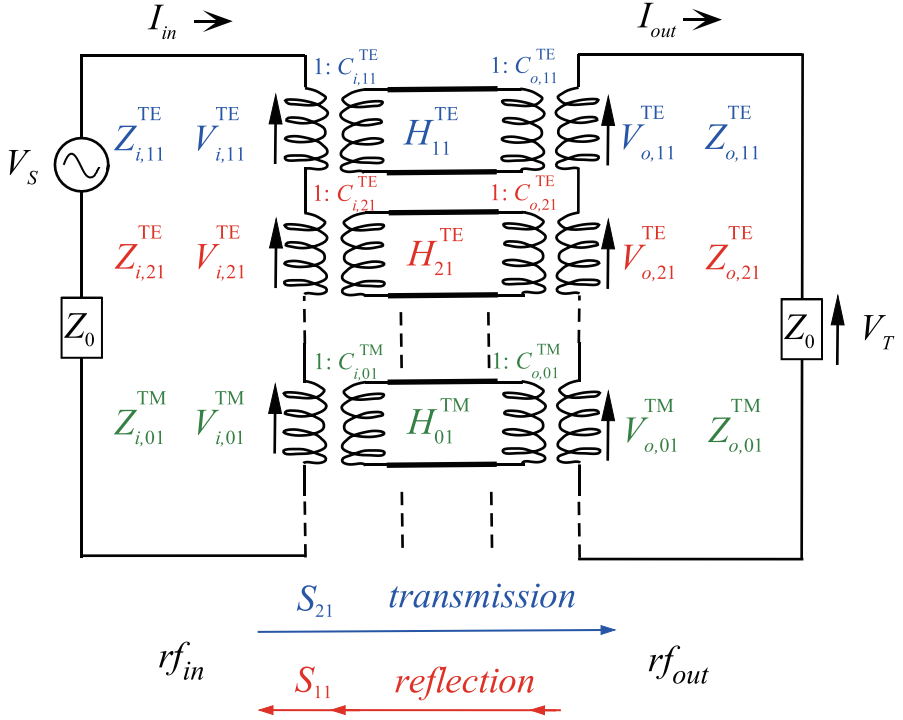

Equivalent circuit model of WBM taking into account electromagnetic couplings between feedthrough electrodes. The couplings for different modes are shown with different colors.

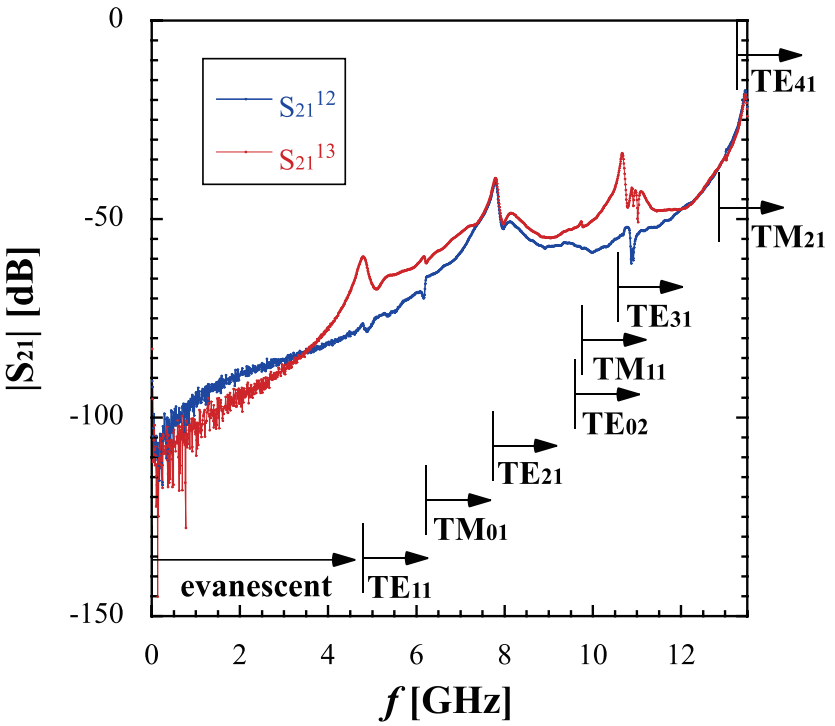

Typical measurement results of amplitude S21 between electrodes No. 1 and No. 2 (blue) [also No. 1 and No. 3 (red)].

Electromagnetic coupling analysis

Detection principle

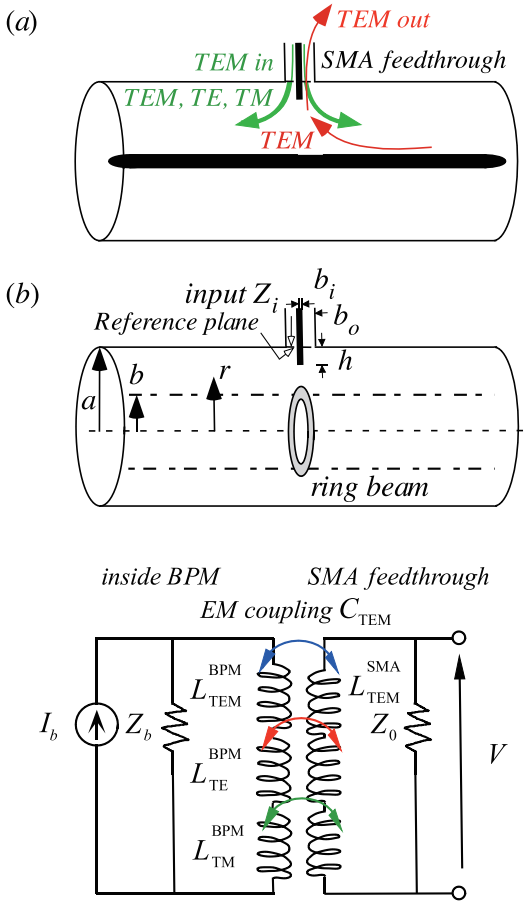

Figure 3:
(a) Schematic drawing of electromagnetic couplings between SMA feedthrough and coaxial structure.

(b) Electromagnetic couplings between SMA feedthrough and a thin ring beam. Inner radius of the coaxial structure: a = 19 mm, ring-beam radius: b, radii of the SMA inner and outer conductor: bi = 0.9 mm, bo = 2.05 mm, and the characteristic impedance of the SMA is Z_0 = 50 **Ω**.

Figure 4: Equivalent circuit of electromagnetic couplings between SMA feedthrough and coaxial structure. The arrows indicate the couplings between TEM (blue), TE (red), and TM (green).

Tsuyoshi Suwada, "Modal Analysis of Electromagnetic Couplings between SMA-Feedthrough Electrode and Beam for Wideband Beam Monitor"; Poster presented at *the 10th International Beam Instrumentation Conference (IBIC2021)*, *Video meeting hosted by PAL, Korea*, Sep. 13-16, 2021 (WEPP12).

Numerical results

Calculations of input impedances for TEM+TE and TEM+TM modes

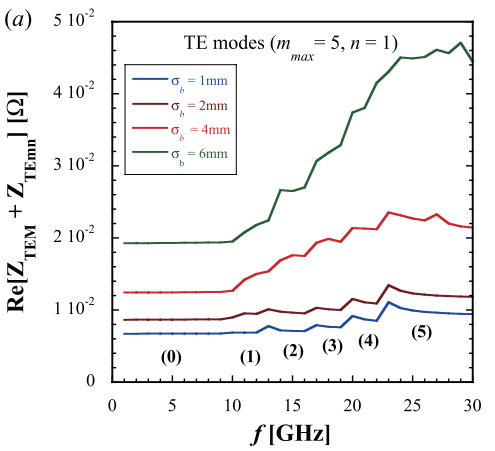

Figure 5:
(a) Variations in the input impedance (TEM+TE modes) as a function of frequency and the beam size.

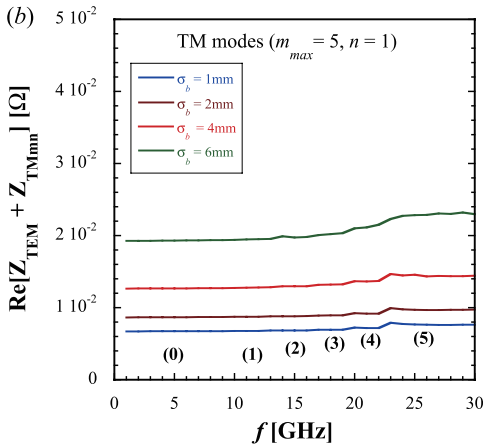

(b) Variations in that (TEM+TM modes) as a function of frequency and the beam size.
The subscripts n and maximum m are fixed to 1 and 5, respectively.
The extruding length is fixed to 1 mm.

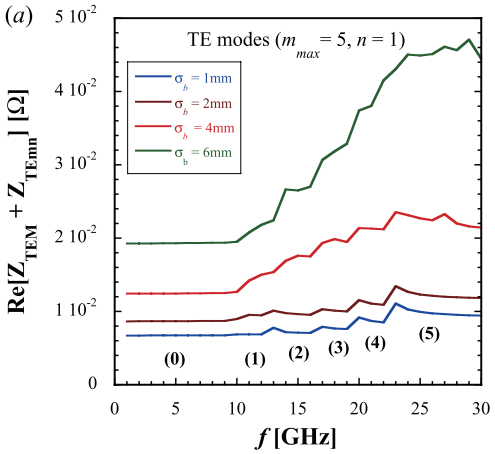

Figure 6:
Variations in the coupling strengths between the TEM modes as a function of frequency and the beam size.

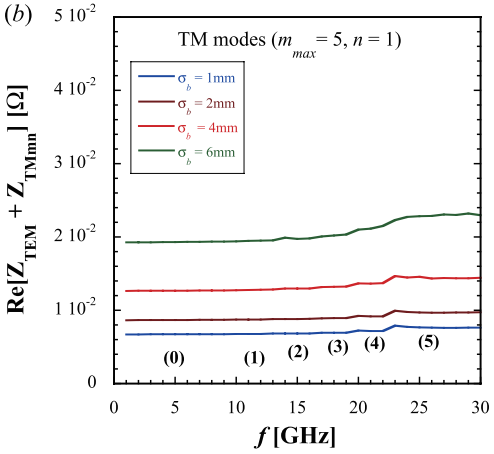

Figure 7:
Variations in the coupling strengths between the TEM modes as functions of frequency and the length. The transverse charge distribution of $\boldsymbol{\sigma_b}$ *= 4 mm is fixed.*

Tsuyoshi Suwada, "Modal Analysis of Electromagnetic Couplings between SMA-Feedthrough Electrode and Beam for Wideband Beam Monitor"; Poster presented at *the 10th International Beam Instrumentation Conference (IBIC2021)*, *Video meeting hosted by PAL, Korea*, Sep. 13-16, 2021 (WEPP12).